University of South Bohemia in České Budějovice

Faculty of Science

Investigating functional p38-MAPK signalling during mouse blastocyst ICM cell-fate maturation

Master's thesis

Bc. Andrea Hauserová

Supervisor: prof. Alexander W. Bruce, Ph.D.

České Budějovice 2023

Master's thesis

Hauserová A., 2023: Investigating functional p38-MAPK signalling during mouse blastocyst ICM cell-fate maturation. Mgr. Thesis, in English - 54 p., Faculty of Science, University of South Bohemia, České Budějovice, Czech Republic.

Annotation

Master's thesis describes the functional role of p38-MAPK signalling during mouse blastocyst ICM cell-fate maturation.

Prohlášení

Prohlašuji, že jsem autorem této kvalifikační práce a že jsem ji vypracoval(a) pouze s použitím pramenů a literatury uvedených v seznamu použitých zdrojů.

V Českých Budějovicích, 13. 4. 2023 …….

Acknowledgment

Above all, I would like to express my sincere gratitude to my supervisor A. W. Bruce for his excellent guidance and help throughout my studies. I am also grateful for his enthusiasm for the project, for his support, encouragement and especially patience. Thank you for the opportunity to perform my master research in your laboratory.

I would like to extend my sincere thanks to my colleagues for their help and advice. My thanks belong especially to Rebecca Collier M.Sc. (Ph.D. student) and Mgr. Martina Bohuslavová (also a Ph.D. student) for imparting to me their knowledge and for never leaving me in a tight spot!

Finally, I wish to thank my parents and siblings and the family as a whole for their continuous support and understanding when undertaking my research and writing my project. I wouldn't have gotten this far without your encouragement.

Abstract

p38-mitogen activated kinases (p38-MAPK) play important roles during early preimplantation development and their activity is required throughout the early developmental period. However, a complete functional and mechanistic understanding of p38-MAPK activity during this time is still lacking. Therefore, we have decided to deepen our knowledge about its role during mouse blastocyst inner cell mas (ICM) cell-fate maturation. Based on our previous findings, pharmacological inhibition of p38-MAPKs (using inhibitor SB220025) between E3.5 and E4.5 that result in a significant reduction in blastocyst diameter/volume and reduced GATA4 expression (*i.e.* significantly impaired numbers of specified and differentiating primitive endoderm cells), we decided to test the hypothesis that the p38-MAPKi phenotype is solely attributable to autonomous ICM mechanisms, that are independent of the outer trophectoderm lineage. To test this hypothesis, we assayed and compared the effect of p38-MAPK inhibition (E3.5-E4.5) on intact cultured blastocysts and on isolated ICMs (using the, newly adopted for our laboratory, immuno-surgery based technique). Our preliminary data strongly indicate similar ICM cell fate maturation phenotypes, suggesting the effect of p38-MAPK signalling in potentiating the primitive endoderm lineage is, largely, ICM autonomous.

Key words: mouse preimplantation developmental stages, the first cell-fate decision, the second cell-fate decision, p38-MAPK, immunosurgery, ICM, TE, PrE, EPI

TABLE OF CONTENT

Glossary of Abbreviations

junction-associated scaffolding angiomotin	AMOT
caudal type homeobox 2	CDX2
epiblast	EPI
fibroblast growth factor	FGF
inner cell mass	ICM
immunosurgery	IS
in vitro fertilization	IVF
primitive endoderm	PrE
receptor tyrosine kinases	RTKs
trophectoderm	TE
transcriptional factors	TF
ultraviolet light	UV
p38 mitogen-activated kinases	p38-MAPK
mitogen activated kinases	MAPK
nuclear envelope breakdown	NEBD
zona pellucida	ZP
zygotic genome activation	ZGA

1 Introduction

1.1 Mouse preimplantation development

1.1.1 An overview of mouse preimplantation embryonic development

The mouse is one of the most widely studied model organisms of mammalian developmental biology. The study of mouse preimplantation embryonic development has helped clarify the major events of human embryo preimplantation development (Cockburn & Rossant, 2010). Mouse preimplantation embryonic development starts with fertilization of an egg by a sperm and extends over 4-5 days until the implantation of the blastocyst into the uterine wall. Once the oocyte is fertilized, there are three rounds of cell cleavage, that lead up to the 8-cell stage embryo. At the 8-cell stage, embryonic polarization and compaction (processes by which all cells of the embryo establish increased baso-lateral cell contacts and an apical domain on the cell–cell contact-free surface, differentially enriched in different polarity factors) are initiated and are followed by possible asymmetric cell divisions, that can give rise to two distinct cell types: outer residing and polarised trophectoderm (TE), which will later form a placenta, and an apolar and pluripotent inner cell mass cells (ICM). The ICM then either specifies as the pluripotent epiblast (EPI), from which the entire foetus is derived, and the differentiating primitive endoderm (PrE), which gives rise to extra-embryonic membranes (Chazaud & Yamanaka, 2016). All three cell lineages are manifest in the late blastocyst stage (E4.5) embryo, in which the ICM is displaced to one pole by a fluid-filled cavity (Figure 1). Cavity formation is initiated by the formation of microlumens (around E3.0), contributed to be the exocytosis of vesicles/vacuoles from the basal membrane of the outer cells and the generation of an osmotic gradient across TE cells caused by sodium/potassium ion exchange of the ATPase, ATP1, localised on baso-lateral membranes. Successful blastocyst cavity formation is essential for further development, not least facilitating embryo hatching from the *zona pellucida* (ZP) to allow uterine implantation (Ryan et al., 2019). Tight junction formation in the outer TE epithelium is important for maintaining cavity integrity and preventing fluid leakage (Mihajlović & Bruce, 2017).

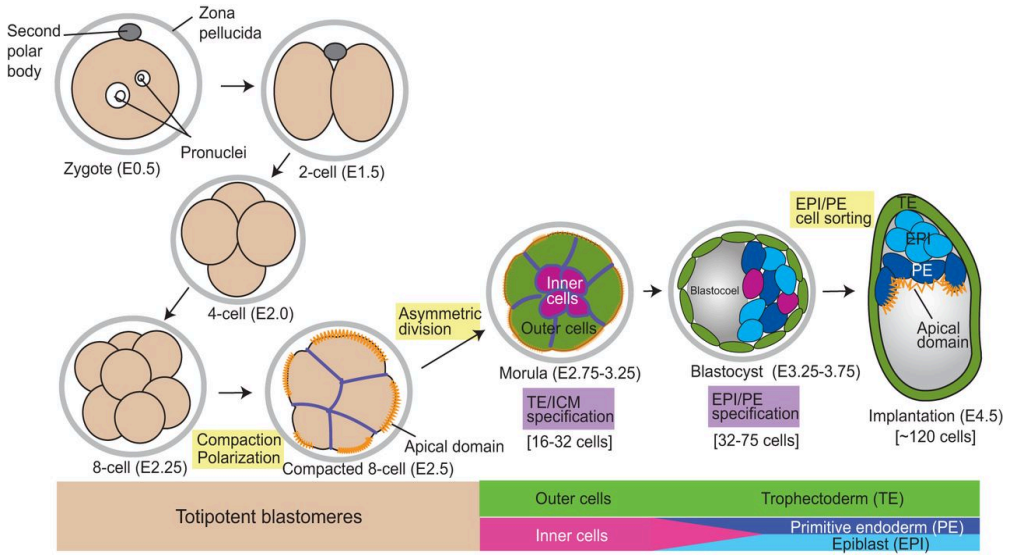

Figure 1: Schematic overview of preimplantation mouse development from the zygote to late blastocyst (E4.5) stage, figure taken from Chazaud et al. 2016.

1.1.2 Development of oocyte

To complete the transformation from an oocyte into an embryo, coordination of several precise processes must occur, that will ultimately allow the uniting of the haploid genomes of each parent into a single diploid zygotic/embryonic genome. Before such union at fertilisation, oocyte/egg development must occur. Primary oocytes remain in the ovary in a quiescent state and are arrested in the prophase of the first meiotic division (prophase I) (White et al., 2018). Primary oocytes require surrounding support cells that provide maternal mRNAs and proteins to the growing oocyte, that will ensure early continuous development post-fertilisation, prior to the activation of the zygotic/embryonic genome (Li & Albertini, 2013). Meiosis, in fully grown primary oocytes, is resumed by hormonal stimulation (characterized by nuclear envelope breakdown, NEBD) and is followed by the formation of the first meiotic spindle. The first meiotic division (meiosis I) is highly asymmetric (segregating half the copied chromosomes into a tiny vestigial cell called the first polar body (Chaigne et al., 2013)), ensured by off-centred positioning of the spindle, which forms approximately in the centre of the cell and then migrates to the nearest cortex. At this stage, there are no signs of polarization, suggesting the spindle axis forms randomly (Brunet & Verlhac, 2011). Spindle migration is ensured by a mechanism of actin polymerization (Yi et al., 2013). After the first polar body is extruded, the meiosis II spindle assembles around the chromosomes and the oocyte remains

arrested at this stage, around ovulation and later potential fertilization, at which point the second polar body is extruded (Mogessie & Schuh, 2017).

1.1.3 Post-fertilisation development

Fusion of an oocyte with a sperm causes the completion of meiosis II and the generation of a second polar body via another highly asymmetric cell division (this time segregating recombined sister chromatids). This fertilisation process also includes translation of maternal mRNAs and facilitates the progression from meiosis to mitosis (White et al., 2018). As the early mouse embryo developmental stages are dependent on mRNAs inherited from the egg, maternal factors control and drive zygote development through the 1-cell stage, when the zygotic genome becomes transcriptionally, yet limitedly, activated (ZGA), with full ZGA occurring at the 2-cell stage. Concomitant with transcriptional activation of the embryonic genome, most maternal mRNA is degraded, although functional proteins synthesized from maternal transcripts can persist until the end of the preimplantation developmental (Zernicka-Goetz et al., 2009).

The newly formed mouse embryo is highly totipotent, with both 2-cell blastomeres capable of independently deriving viable blastocysts and certainly until the 8-cell stage (and even the early blastocyst stage), it is considered that each blastomere retains the ability to generate all three lineages (TE, PrE, EPI) (Posfai et al., 2017; Suwińska et al., 2008); moreover the preimplantation developmental period is highly flexible and adaptable, with the ability to withstand removal or addition of blastomeres and compensate the viable blastocyst developmental programme (Mihajlović & Bruce, 2017). However, individual cell totipotency gradually disappears in the course of blastocyst development (Casser et al., 2017). The first morphological changes in preimplantation mouse embryo development can be observed at the 8-cell stage, where two key morphogenetic processes take place; compaction and polarization (Chazaud & Yamanaka, 2016). Compaction involves the formation of adherens junctions at cell-to-cell contact sites (*i.e.* along inter-facing basolateral membranes) and results in a structure called the morula (Mihajlović & Bruce, 2017); the proteins E-cadherin and β-catenin are essential for compaction and later blastocyst formation (de Vries et al., 2004). Around the same period of compaction, 8-cell stage blastomeres undergo intra-cellular polarization, (Figure 2). Polarization is initiated along a blastomere's radial axis (with respect to the embryo as a whole) and results in enrichment of specific polarity factors (proteins PAR3, PARD6 and atypical PKC - aPKC) at the cell contactless apical, and contacted basolateral (*e.g.* PAR1 and

SCRIB) membrane domains (Chazaud & Yamanaka, 2016). Following compaction and initiation of polarization, 8-cell stage embryos undergo another two rounds of cleavage cell division and transfer first to the 16-cell and then 32-cell stages. Such divisions are orientated by the position of the blastomere cleavage plane. If the cell division occurs at an angle perpendicular to its axis of polarity, its two daughter cells will retain polarity (by means of both inheriting part of the contactless apical domain) and will remain on the outside of the embryo; termed a symmetric division. However, if cells divide in parallel to their axis of polarity, one polarized outer-daughter cell (inheriting most if not all the apical domain) and one apolar cell inside of the embryo (primarily inheriting basolateral membranes) are generated; termed an asymmetric division. Although, most divisions are a variant of intermediary oblique divisions that generate daughters with unequal contactless and polarised apical domains, that via mechanisms of differential actomyosin contractility, internalise or remain on the surface of the embryo (reviewed in Bruce and Mihajlovic 2017). Consequently, at the 32-cell stage, the embryo has organized cells to either apolar inside or polarised outside positions, which helps assists the formation/specification of the TE and ICM (*i.e.* EPI and PrE) lineages (Cockburn & Rossant, 2010).

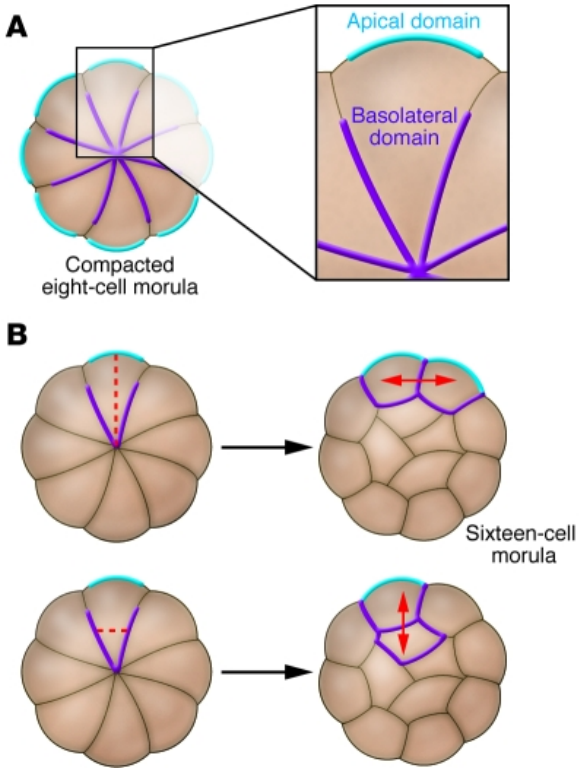

Figure 2: Schematic depiction of apical-basolateral polarization in the mouse preimplantation morula. **(A)** Schema of establishment of the apical-basolateral membrane domains **(B)** Blastomeres of the morula can symmetrically (upper) asymmetrically (lower) divide to yield outer-polarised and inside apolar daughter cells (from the 8-cell to 16- cell, and 16-cell to 32-cell, transitions). Taken from Cockburn et al. 2010.

1.2 The first cell lineage decision

The first cell-fate decision is between outer and differentiating trophectoderm (TE) cells and pluripotent inner cell mass (ICM), which further specifies/differentiates into the EPI and PrE cell lineages (starting from around the E3.5 stage and culminating at the E4.5 late blastocyst stage). There are two models, describing how cells decide their fate as TE or ICM. According to the "inside-outside" model, cells on the outside and inside are exposed to different levels of cell contact and different microenvironments, and this positional information is translated into an appropriate TE or ICM cell-fate. The second model, the "cell polarity model", is based on inheritance of apical basolateral polarity in outer cells, that is translated into a TE fate. According to this model, the presence or absence of cell polarity is considered a key factor governing differentiation towards an outer TE fate or specification as pluripotent ICM (Cockburn & Rossant, 2010). As detailed below, this model is now more favoured (in terms of differential activation of the Hippo-signalling pathway in inner and outer cells), although

aspects of both models hold true and appear inter-dependent (as reviewed, according to the revised "polarity-dependent cell-positioning" model) (Mihajlović & Bruce, 2017).

The specification of the TE and ICM lineages is marked by coordinated expression of a group of transcription factor (TF) genes. The *Caudal type homeobox 2* (*Cdx2*) gene is TE-specific and required for TE maintenance and development. The pluripotency marker genes *Octamer-binding protein 3/4* (*Oct4*, also known as *Pou5f1*), *Nanog* and *SRY-box containing gene 2* (*Sox2*) are important in establishing ICM pluripotent cell fate. In mouse embryos, starting at the 8-cell stage, the level of *Cdx2* expression varies between blastomeres, but becomes restricted to only the outer cells of the early (E3.5) blastocyst, when the specification of TE becomes irreversibly committed (Posfai et al., 2017). Markers for the ICM lineages display the inverse expression, only being expressed in inner cells by the blastocyst stage. The repression of *Cdx2* transcription by OCT4, NANOG and SOX2 reinforces these spatially distinct expression patterns, as does autoregulation of *Oct4* and *Cdx2* gene transcription (Cockburn & Rossant, 2010).

The establishment of such necessary gene expression patterns underpinning the first cell fate decision is largely contributed by differential activity of the Hippo/YAP signalling cascade (Menchero et al., 2017). This pathway was first described in *Drosophila* as a cell growth regulator, acting via a regulated nuclear localization of a transcriptional coactivator protein called Yorkie (Yki). An analogous Hippo/YAP network exists in mammals and includes the same core components as identified in *Drosophila*, but under different names (Shuguo & Kenneth, 2016), and acts as a sensing mechanism for local cellular environments, cellular density, cellular positioning and stiffness of extra-cellular matrices. It has been shown that the Hippo/YAP pathway plays an important role in the establishment of the TE and the ICM in the mouse preimplantation embryo, as transgenic embryos lacking the Hippo-related transcription factor gene *Tead4* fail to both cavitate and create a mature TE layer (as would be marked by CDX2 expression) and therefor are unable to implant (Wicklow et al., 2014). Similarly, YAP1 (YAP – and its paralog TAZ) has been shown to be a transcriptional co-activator for TEAD4, together forming a complex that upregulates TE specific gene expression (Chazaud & Yamanaka, 2016). However, as YAP localisation between the nucleus and cytoplasm (and *vice versa*) is regulated a phosphorylation-dependent manner, the transcriptional regulatory output of TEAD4 can be modulated. Hence, when YAP is unphosphorylated it can translocate to the nucleus and partner with TEAD4 to activate TE-specific gene expression (*e.g. Gata3* of *Cdx2*) or it can be phosphorylated, by active Hippo-

signalling-related LATS kinases, leading to its cytoplasmic sequestration and failure to form a TEAD4-YAP, and TE gene, transcriptional activating complex (Nishioka et al., 2009). This differential Hippo/YAP signalling output is required for a brief period 8- to 32-cell stages to establish distinct gene expression patterns in the emerging ICM and TE lineages (Lorthongpanich et al., 2013).

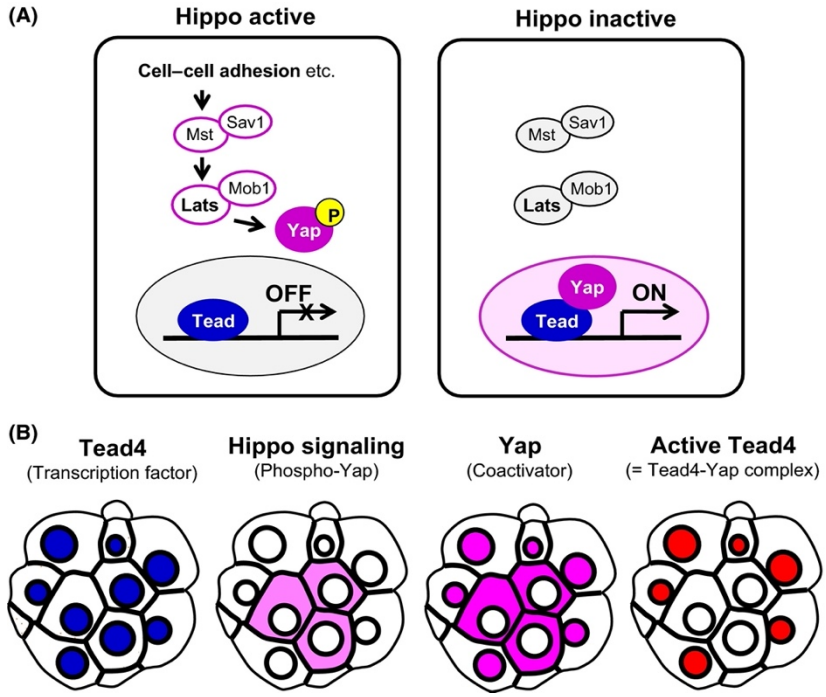

Figure 3: Schematic representation of the roles and regulations of differential Hippo-signalling activity during mouse preimplantation development, taken from Sasaki 2017.

The differential activation of the Hippo-signalling pathway in spatially distinct TE (off) and ICM (on) lineages is regulated by localisation of junction-associated scaffolding Angiomotin (AMOT) proteins (Chazaud & Yamanaka, 2016). In apolar inner cells, AMOT is localized at adherens junctions, where it interacts with two other Hippo-pathway components, LATS1/2 and NF2 (Neurofibromin 2). This promotes LATS1/2 kinase mediated and stabilising phosphorylation of AMOT that in turn permits LATS1/2 to phosphorylate other substrates, including YAP causing its cytoplasmic retention. Conversely, AMOT sequestration to the polarised apical domain of outer cells, prevents this association and unphosphorylated YAP enters the nucleus to facilitate TEAD4-mediated TE gene transcription (Hirate et al., 2013). Figure 3 (Sasaki, 2017) summarises the regulatory roles of Hippo signalling during preimplantation mouse development and in the emerging outer-TE and inner-cells by the early blastocyst stage.

1.3 The secondcell lineage decision

Shortly after the execution of the first cell-fate decision (when the E3.5 stage blastocyst has segregated outer and inner cell lineages and an expanding cavity has been established), ICM cells begin their segregation into the two lineage options; differentiating primitive endoderm (PrE), that gives rise to extra-embryonic tissues, and the pluripotent epiblast (EPI), from which all foetal tissues are derived (Chazaud & Yamanaka, 2016).

The earliest exclusive expression marker proteins for the EPI and PrE lineages are the transcription factors NANOG and GATA6, respectively (Chazaud et al., 2006). However, they are co-expressed in all 32-cell stage ICM blastomeres, after which individual cells maintain expression of either NANOG (to contribute to the EPI lineage) or GATA6 (for the PrE lineage), at the expense of the other marker. This initiated ICM expression pattern of randomised NANOG or GATA6 positive EPI and PrE progenitors, respectively, is called the "salt and pepper" pattern and commences around E3.75 (Chazaud & Yamanaka, 2016). According to various cell lineage tracing and live cell tracking analyses (Chazaud et al., 2006; Kurimoto et al., 2006; Plusa et al., 2008), the initiation of the "salt and pepper" expression pattern occurs in individual ICM cells allochronicly, ranging from ~E3.0 to E3.75 (Bessonnard et al., 2014; Plusa et al., 2008). Hence, even ~E3.75 a few ICM cells continue to co-express both NANOG and GATA6 (Chazaud & Yamanaka, 2016). The mechanism controlling the "salt and pepper" specification process is considered via selective mRNA decay rather than selective increases in transcription, because expression levels of *Nanog* and *Gata6* mRNA are relatively high from as early as the 8-cell stage (Guo et al., 2010). Nevertheless, there still appears to exist a mutual antagonism between *Nanog* and *Gata6* gene expression, as *Gata6* mutant embryos display pan-ICM expression of NANOG, without any PrE marker gene expression; consistently, *Nano* mutants present ICM cells all expressing GATA6 (Bessonnard et al., 2019; Schrode et al., 2014).

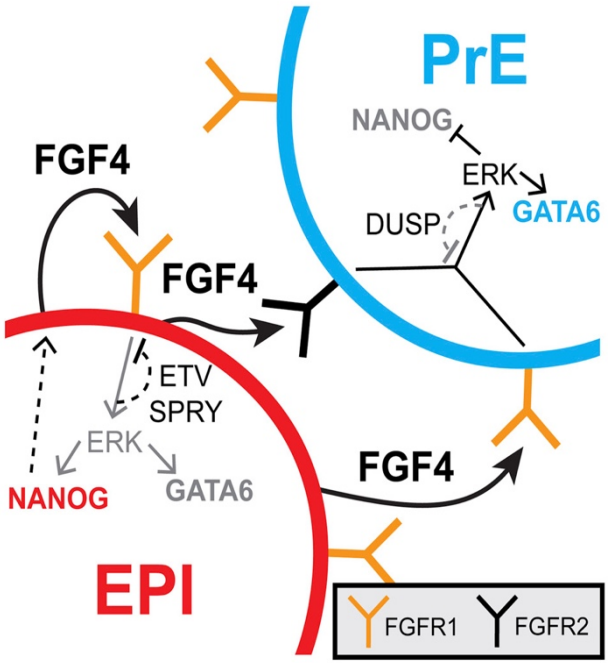

Figure 4: Model of FGFR1 and FGFR2 expression in mouse blastocyst EPI and PrE progenitors of the mouse blastocyst ICM. Taken from Kang et al., 2017.

The Fibroblast growth factor (FGF) signalling pathway plays an important role during ICM cell-fate specification and PrE lineage differentiation (Chazaud & Yamanaka, 2016). In this context the FGF pathway has two signalling components, the ligand encoded by *Fgf4* and its receptors encoded by *Fgfr1* and *Fgfr2*, that together with the mutual repression of NANOG-GATA6 expression, are needed for correct ICM cell lineage specification (Chazaud & Yamanaka, 2016; Guo et al., 2010; Kang et al., 2017). The currently described model for regulation by FGF4, and downstream mitogen-activated protein kinases (MAPK) signalling pathway activity, falls on the reciprocal expression of the FGF4 ligand with provided refinement in EPI and PrE progenitors provided by FGFR1 and FGFR2 receptor expression. At the E3.25 stage, before cells are anticipated to have initiated the second cell fate decision, *Fgf4* is the first gene to exhibit a heterogenous expression profile across cells of the ICM and is thereafter only expressed in cells with an EPI-biased fate (Ohnishi et al., 2014). *Fgfr2* gene expression succeeds and contradicts the expression pattern and is detected in PrE-biased cells by the E3.5 stage, whereas all ICM cells express *Fgfr1* (Guo et al., 2010; Ohnishi et al., 2014). If both FGFR1/2 receptors or downstream components of the activated MAPK pathway (*i.e.* MEK1/2) are genetically ablated and/or pharmacologically targeted by small-molecule inhibitors, PrE differentiation is blocked and all ICM cells adopt an EPI identity (Chazaud et

al., 2006; Kang et al., 2013; Yamanaka et al., 2010). Conversely, blastocyst exposure to exogenous recombinant FGF4 drives all ICM cells, and not just those expressing the *Fgfr2* gene, to adopt a PrE fate; meaning all ICM cells have the capacity of responding to FGF4 stimulation (Yamanaka et al., 2010). Figure 4, taken from Kang et al., 2017, describes a mechanistic model, from within this context, by which pan-ICM expressed FGFR1 enables the maintenance of GATA6 levels in PrE-biased cells (also marked by FGFR2 expression) and also enables the expression of NANOG in EPI-biased cells; therefore sustaining expression of FGF4 ligand in order to drive the paracrine segregation of EPI and PrE fated cells as the blastocyst ICM matures (Kang et al., 2017; Molotkov et al., 2017).

After initial specification of EPI and PrE progenitors, PrE cells initiate a sequential activation of other marker proteins, such as SOX17, GATA4, DAB2 and PDGFRα, indicating a progressively more differentiated state. Although it is known that GATA6 plays key role in PrE specification, there are other signalling factors and pathways which also act during the subsequent stages of PrE maturation (Chazaud & Yamanaka, 2016). For example, in *Nanog* mutant embryos, where GATA6 is expressed in all ICM cells, the expression of the later SOX17 and GATA4 PrE markers is diminished; suggesting GATA6 expression alone is not sufficient to promote complete PrE maturation (Frankenberg et al., 2011; Messerschmidt & Kemler, 2010; Silva et al., 2009). An important EPI marker is SOX2, yet it is also essential for PrE maturation (although not for EPI/PE specification). This is because SOX2 supports ongoing PrE differentiation via a non-cell autonomous mechanism of ensuring EPI-biased cells continue to express and secrete the FGF4 ligand; at the same time SOX2 maintains the expression of pluripotency genes in the ICM and the eventual formation of the EPI lineage. Therefore SOX2 holds the position as a nodal TF, by maintaining the expression of other important gene, such as *Oct4* or *Fgf4*, that are required for the segregation of the specified blastocyst ICM lineages (Chazaud & Yamanaka, 2016).

1.4 Receptor tyrosine kinases

Receptor tyrosine kinases (RTKs) are a subclass of tyrosine kinases located as plasma membrane embedded cell surface receptors that bind extracellular ligands/factors that can activate various signalling cascades; such as MAPK/ERK1/2 pathway. Thus, they are central to mediating cell-cell communication and control a wide range of complex biological functions, such as cell growth, motility, differentiation and metabolism (Du & Lovly, 2018). Members of the RTK super-family include several important subgroups of receptors such as

fibroblast growth factor receptors (FGFRs), epidermal growth factor receptors (EGFRs), vascular endothelial growth factor receptors (VEGFRs), and platelet-derived growth factor receptors (PDGFRs); all implicated in a broad range of cellular responses that include embryonic development, angiogenesis, oncogenesis, and metabolism.

RTKs are also involved in the differentiation of preimplantation mammalian embryonic cells, related to the first differentiation events (*i.e.* the distinction of TE/ICM and the later segregation of the ICM into EPI and PrE). For example, pharmacological inhibition of ERK2 (an RTK effector kinase acting downstream of Ras-MAPK) at the 8-cell stage results in a significant decrease in CDX2 protein expression in resulting outer cells; indicating Ras-MAPK signalling as a contributory mechanism promoting TE cell-fate in the early embryo (Menchero et al., 2017). Regarding the segregation of EPI and PrE within the ICM; genetic null mutant embryos without *Grb2*, an RTK-associated adaptor protein, are more likely to fail to differentiate later endoderm lineage derivatives (Cheng et al., 1998). Additionally, *Grb2* mutant embryos do not express *Gata6* and express *Nanog* throughout the ICM rather than the normal salt-and-pepper distribution (Chazaud et al., 2006). During different preimplantation stages, the requirement of RTK signalling to sustain *Gata6* expression is not permanent. This is supported by the differing effects of RTK inhibitors (Mek inhibitor PD0325901 or Fgf receptor inhibitor PD173074) depending on the timing of administration (Frankenberg et al., 2011; Nichols et al., 2009). For example, when RTK signalling is inhibited from the morula stage, *Gata6* is not expressed (either in the presence or absence of *Nanog* in the later blastocyst stages), reproducing the *Grb2*$^{-/-}$ null phenotype. However, if the inhibition is administrated after embryonic cavitation, *Gata6* is only expressed in the absence of *Nanog* (Menchero et al., 2017). Thus, RTKs are important for initiating *Gata6* expression but maintenance of *Gata6* is RTK-independent and requires *Nanog* downregulation. Interestingly, if RTK signalling is inhibited in both wildtype and *Gata6* mutant embryos, NANOG expression levels are upregulated, suggesting a double role for this pathway; promoting PrE fate and maintaining *Nanog* expression levels within a physiological range (Schrode et al., 2014).

1.4.1 p38 mitogen-activated protein kinases (p38-MAPKs)

p38-MAPKs are the effector proteins of pathways mediating varied cellular processes, such as cell proliferation, growth, differentiation and cell death (Natale et al., 2004). They can, and were classically, characterized as stress-induced kinases, activated by various cellular processes and stimuli; including inflammatory cytokines, lipopolysaccharides (LPS),

ultraviolet light (UV), and growth factors (Petersen et al., 2016). p38-MAPKs also regulate preimplantation development and their activity is required throughout the early development period of the mouse embryo (Bell & Watson, 2013; Bora et al., 2019; Natale et al., 2004); expanded below.

p38-MAPKs represent a subgroup of the wider MAPK superfamily (including ERK1/2, JNK and ERK5) and compromise four isoforms encoded by different genes; p38-MAPKα (MAPK14), β (MAPK11), γ (MAPK12), and δ (MAPK13) which share more than 60% amino acid identity (Natale et al., 2004). All isoforms act through multiple substrate effectors that include several transcription factors, MAP kinase-activated protein kinase-2 (MK2) and p38-regulated/activated protein kinase (PRAK); PRAK and MK2 are preferentially targeted by active p38-MAPK α or β (Natale et al., 2004). The best described isoform, that is also expressed in most cell types, is p38α (Remy et al., 2010). The p38-MAPKs can be further divided into two subgroups, the first containing p38α and p38β (75% amino acid identity in mouse) and the second group containing p38γ and p38δ (62% amino acid identity in mouse) (Remy et al., 2010). As referenced above, p38-MAPKs can be activated via wide variety of environmental stress or inflammatory cytokine stimuli, however, these converge onto only two known directly activating p38-MAPK MAPK kinases, MKK3 and MKK6; that act via phosphorylation of the TGY motifs in the activation loop of p38-MAPK isoforms. Both MKK3 and MKK6 specifically activate p38β and p38γ in response to varied environmental stress stimuli. MKK6 can phosphorylate/activate p38γ in response to the cytokine tumour necrosis factor-α (TNFα) and MKK3 can activate p38δ upon exposure to UV radiation (Remy et al., 2010). Such mechanisms of p38-MAPK activation are canonical and once active p38-MAPKs are estimated to (collectively) phosphorylate and regulate around 200-300 substrates/proteins, including transcriptional factors and chromatin remodelers (Cuadrado & Nebreda, 2010).

All four p38-MAPK isoforms are known to be expressed during preimplantation development of the mouse embryo (Bora et al., 2021; Natale et al., 2004), particularly at 8-cell stage and in relation to promoting development of the blastocyst (Remy et al., 2010). The pharmacological inhibition of p38-MAPKα/β (using the inhibitor, SB203580) results in reversible arrest of preimplantation development (by blocking the H_2O_2-induced endothelial microfilament responses), directly implicating the involvement of p38-MAPK activity for successful preimplantation development of the mouse embryo (Cirillo et al., 2002; Davidson & Morange,

2000; Huot et al., 1997; Natale et al., 2004). Moreover, if p38-MAPK pharmacological inhibition is given prior to blastocyst cavity formation (between E1.5 to E3.5), embryos enter a reversible developmental arrest around the late morula stage (~32 cells) with or without a deformed cavity; indicating the importance of p38-MAPK activity to TE formation and function (Yang et al., 2015 +*references below*). p38-MAPK function has also been implicated as a potential regulator of filamentous actin in the preimplantation embryo; indicating its involvement during embryo compaction (Natale et al., 2004). Furthermore, p38-MAPKs are important in the establishing of the trans-epithelial (TE) ionic gradient that facilitates the formation of the fluid-filled blastocyst cavity; important for successful blastocyst expansion, hatching and uterine implantation (Giannatselis et al., 2011). For example, chemical inhibition of p38-MAPK (using the inhibitor SB220025) results in significant reductions in blastocyst diameter/volume due to aquaporin (AQP3) and Na^+/K^+ ATPase dysregulation and the disruption of TE tight junction formation (Bell & Watson, 2013). In work from our laboratory, we have identified p38-MAPK activity (also using a chemical inhibitor based approach) as necessary between E3.5 to E4.5 for appropriate PrE specification and differentiation, but not EPI specification, in the mouse blastocyst ICM (Thamodaran & Bruce, 2016). In a subsequent work we also reported p38-MAPK activity is required to negate amino acid deprivation induced oxidative stress, and the associated blastocyst developmental and ICM cell-fate defects, by facilitating increased antioxidant enzyme-related gene expression (Bora et al., 2019). More recently, our laboratory has uncovered more of the mechanistic basis of the role of p38-MAPK in blastocyst PrE lineage specification and differentiation; particularly related to p38-MAPK role as a regulator of protein translation (and regulator of multiple ribosome biogenesis associated factors and rRNA processing); during an early window of blastocyst maturation (E3.5 -E3.5+7h) that acts as a primer for PrE specification from the uncommitted ICM state, allowing subsequent differentiation (Bora et al., 2020).

In our laboratory research, addressing the mechanisms of p38-MAPK pathway inhibition (related to regulation of protein translation and PrE specification/differentiation), it was confirmed that p38-MAPK inhibition (between E3.5-E4.5) also impairs blastocyst cavity expansion (Bora et al., 2020). According to Ryan et al. 2019, chemical modulation (using Ouabain – an inhibitor of the ATP1 channel, that is responsible for cavity fluid accumulation) and mechanical modulation of blastocyst cavity size during early blastocyst maturation (E3.5-E4.0) results in reduced levels of PrE specific marker protein expression (*e.g.* GATA4 – albeit assayed at E4.0). Our results describing PrE differentiation defects, which were caused by

inhibition of p38-MAPK (Bora et al., 2019; Thamodaran & Bruce, 2016) resemble those in mechanically deflated blastocysts; *i.e.* representing reduced GATA4 expression but normal specification of the EPI in both cases (expressing either NANOG or SOX2 alone) (Ryan et al., 2019). Based on such collective observations, inhibition of p38-MAPK that results in impaired numbers of blastocyst PrE differentiating cells, may e (at least in part) mediated by an induced TE defect; as such TE defects could result in insufficient cavity expansion, with the potential for knock-on consequences for PrE specification and differentiation (Bora et al., 2020). Therefore, we wanted to test our hypothesis if p38-MAPKi PrE differentiation induced phenotypes are mediated by a TE defect, or if the p38-MAPKi effect is ICM specific. To test this hypothesis, the inhibition of p38-MAPK has to be performed exclusively on ICMs. To obtain a large number of ICMs in a short period of time, a new technique called immunosurgery (IS) had to be introduced into the laboratory. This technique makes use of antibodies that bind to the outer trophectoderm cells but not to the cells of the ICM. After exposure of the embryo to complement factors (a mixture of proteins that are part of the immune system) the cells that have bound antibodies are destroyed, as the complement attaches to the antibodies, leaving the ICMs that can subsequently be cultured (with or without chemical inhibition).

2 Thesis aims

- To learn “Immunosurgery/IS”: ICM isolating technique.
- Quantification and analysis of specific blastocyst cell lineage marker gene expression (TE, PrE and EPI) with and without p38-MAPK inhibition on intact bouse blastocysts and immunosurgically isolated ICM’s using immunofluorescence (IF) confocal microscopy.
    - Our hypothesis is, if p38-MAPKi PrE differentiation induced phenotype is ICM specific/autonomous, we should observe similar PrE specification/differentiation defects in immunosurgically isolated ICM’s as previously reported intact blastocysts; a lack of effect would implicate the TE/cavity based mechanism.

3 Materials and methods

3.1 Mouse lines and embryo culture

To obtain 2- and 8-cell stage mouse preimplantation embryos and blastocysts for experimentation, F1 female hybrid mice (derived from C57BL6/J (female) x CBA/W (male) crosses) were superovulated by peritoneal injection with 7.5 IU PMSG (pregnant mare serum gonadotrophin extract; Folligon MSD Animal Health) and 48 hours later with 7.5 IU hCG (human chorionic gonadotrophic hormone; Sigma-Aldrich® cat. #CG10) and transferred into a cage with one F1 male to mate overnight. To obtain 2-cell stage embryos, females were killed approximately 48 hours after hCG injection (to obtain 8-cell stage, 67 hours after hCG injection) and fallopian tubes (after dissection) were immediately transferred into M2 media (pre-warmed at 37°C for at least 2-3 hours). To obtain freshly flushed blastocysts, females were killed 90-96 hours after hCG injection by cervical dislocation and fallopian tubes with the uterus attached were then transferred into M2 media (also pre-warmed at 37°C). 8-cell stage embryos (E2.5) were isolated in M2 media and cultured in KSOM media (EmbryoMax® KSOM Mouse Embryo Media; cat. #MR-020P-5F – pre-warmed at 37°C and pre-equilibrated in a 5% CO_2 atmosphere) with amino acid (AA) supplementation (KSOM +AA; Gibco MEM Non-Essential Amino Acids Solution (100x) used at a working concentration of 1x, cat. #11140035 and Gibco MEM Amino Acids Solution (50×) used at a working concentration of 0.5x, cat. # 11130036). Embryos were cultured in KSOM+AA micro-drops (approx. 15µl) prepared in 35mm tissue culture dishes, overlaid with light mineral oil (Irvine Scientific. Cat. #9305) and then maintained in 5% CO_2 incubators at 37°C until the appropriate developmental stage. Freshly flushed blastocysts (E3.5) were used immediately after isolating in M2 media for experiments (described below). All experiments performed on mice were carried out in accordance with EU directive 2010/63/EU.

3.2 Inner cell mass (ICM) isolation by immunosurgery

For immunosurgery (IS), freshly flushed blastocysts and blastocysts cultured from 8-cell stage were used. Before IS, collected/cultured blastocysts were pipetted into pre-warmed drops of acid Tyrode's Solution (Sigma-Aldrich® cat. #T1788) to remove the ZP. When the ZP was no longer visible, blastocysts were transferred into drops of pre-warmed M2 media and incubated for 15 minutes. Blastocysts were then incubated in anti-mouse serum (1:2 in M2 media, Sigma Aldrich) for 40 minutes and then incubated in guinea pig complement (1:4 in M2 media, 30 minutes; EMD Millipore Corp., cat# 3816047) to lyse outer-trophectoderm (TE)

cells; guinea pig complement solution in M2 has lower stability, therefore it is used from frozen stocks 20 minutes prior to use to maintain stability. To obtain isolated inner cell mass (ICM), lysed TE cells were removed by mouth pipetting using a narrow glass pipette with a diameter approximating that of the ICM, in regular M2 media drops (all employed treatments were conducted with pre-warmed and equilibrated 37^{o}C media, including incubation period were appropriate).

3.3 Embryo and isolated ICM culture under chemical inhibition

Embryos with a blastocyst cavity that occupied approximately 50% of the total embryonic volume at E3.5, were moved to either inhibitory or control conditions and cultured for a further 24 hours (to the E4.5 stage). Inhibition of p38-MAPK was performed using SB220025 (Calbiochem® cat. #559396; dissolved in dimethyl sulfoxide/DMSO) at a 20μM working concentration in KSOM+AA culture medium; an equivalent volume of DMSO solvent was used in the control culture conditions.

Immuno-surgically isolated ICMs, prepared from blastocysts 92–96 hours post-hCG injection, were moved to either inhibitory or control culture conditions. Inhibition of p38-MAPK on ICMs was performed using also SB220025 (Calbiochem® cat. #559396; dissolved in dimethyl sulfoxide/DMSO) at a 5μM working concentration in KSOM+AA culture medium; an equivalent volume of DMSO solvent (as a control culture condition) was used. After 12 hours of inhibition, ICMs were transferred and washed in drops of regular/non-supplemented KSOM+AA culture medium and incubated for another 12 hours (to the E4.5 equivalent stage); ICMs in control condition were also washed and transferred to KSOM+AA drops in an identical manner.

3.4 Blastocyts and ICM fixing and imunofluorescence staining

After required *in vitro* culturing, embryos/isolated ICMs were briefly washed in pre-warmed KSOM+AA media and then pipetted into pre-warmed drops of acid Tyrode's solution (Sigma-Aldrich® cat. #T1788, diluted in mixture of salts in water) to remove the ZP. After removing the ZP, embryos were immediately washed through pre-warmed drops of M2 media and fixed with 4% paraformaldehyde (Santa Cruz Biotechnology, Inc. cat. # sc-281692), diluted in phosphate buffered saline (PBS), for 15 minutes (10 minutes for ICM) at room temperature. Blastocyst and ICMs were then washed in 3 drops of PBS containing 0.05% TWEEN® 20 (PBST; Sigma-Aldrich cat. #P9416) for 20 minutes. Blastocysts were transferred to a 0.5% solution of Triton X-100 (Sigma-Aldrich® cat. #T8787), in PBS, to permeabilize for 20

minutes at a room temperature; ICMs were transferred to a 0.1% solution of Triton X-100 (Sigma-Aldrich® cat. #T8787) in PBS, to permeabilize for 15 minutes at a room temperature. Blastocysts and ICMs were then washed again in 3 drops of PBST for 20 minutes. Blocking was performed in 3% bovine serum albumin (BSA; Sigma-Aldrich® cat. #A7906) in PBST for 30 minutes at 4°C, followed by primary antibody incubation (at the desired dilution in blocking buffer BSA) overnight or for at least for 16 hours at 4°C. Embryos were then washed in 3 drops of PBST for 20 minutes and blocked in BSA-PBST for 30 minutes at room temperature. Suitably diluted (in blocking buffer) fluorescently conjugated secondary antibodies were then used to stain the embryos by room temperature incubation for 60 minutes (in the dark). The immuno-fluorescently (IF) stained embryos were then mounted in DAPI-containing VECTASHILED® medium (Vector Laboratories, Inc. cat. #H-1200), placed under cover slips on recessed glass-bottomed 35mm culture plates and incubated at 4°C for 30 minutes in the dark, prior to fluorescent confocal microscopy mediated image acquisition. The commercial details of the primary and secondary antibodies used, and their employed dilutions/concentrations are summarized in table 1.

Tab. 1: An overview of used antibody and their dilution

Antibody against	Type	Target	Host/Isotype	Manufacturer	Dilution used
NANOG	Primary (monoclonal)	Mouse	Rat/IgG2	Thermo Fisher (14-5761-80)	1:200 in PBST (3% BSA)
GATA-4	Primary (polyclonal)	Mouse, rat and human	Rabbit / IgG	Santa Cruz Bio. (sc-9053)	1:200 in PBST (3% BSA)
CDX2	Primary (monoclonal)	Conserved	Mouse / IgG1, kappa	BioGenex (MU392A-5UC)	1:200 in PBST (3% BSA)
SOX2	Primary (monoclonal)	mouse	Mouse	Santa Cruz Bio. (cs-365823)	1:200 in PBST (3% BSA)
Donkey anti-Rat IgG (H+L) Highly Cross-Adsorbed Secondary Antibody, Alexa Fluor 488	Secondary (polyclonal)	Rat	Donkey / IgG	Thermo Fisher (A-21208)	1:500 in PBST (3% BSA)
Donkey anti-Rabbit IgG (H+L) Highly Cross-Adsorbed Secondary Antibody, Alexa Fluor 555	Secondary (polyclonal)	Rabbit	Donkey / IgG	Thermo Fisher (A-31572)	1:500 in PBST (3% BSA)
Donkey anti-Rabbit IgG H&L (Alexa Fluor® 647)	Secondary (polyclonal)	Rabbit	Donkey / IgG	Abcam (ab150075)	1:500 in PBST (3% BSA)
Donkey anti-mouse IgG H&L (Alexa Fluor647)	Secondary (polyclonal)	mouse	Donkey / IgG	Abcam (ab 150107)	1:500 in PBST (3% BSA)

Isolated ICMs and blastocysts that were cultured in both p38-MAPK inhibited and control conditions with DMSO, were IF-stained using a combination of two or three indicated primary antibodies (as described in the results) and respective/corresponding fluorescently-conjugated secondary antibodies, as required for specific experiments (summarised Table 2).

Table 2: An overview of antibody combinations employed in ICM/blastocyst immuno-fluorescent staining.

	Antibody combination used					
	Primary 1	Primary 2	Primary 3	Secondary to primary 1	Secondary to primary 2	Secondary to primary 3
1	NANOG (rat)	GATA4 (rabbit)	-	Donkey rat (488)	Donkay rabbit (647)	-
2	NANOG (rat)	CDX2 (mouse)	-	Donkey rat (488)	Donkey mouse (647)	-
3	GATA4 (rabbit)	CDX2 (mouse)	-	Donkey rabbit (555)	Donkey mouse (647)	-
4	NANOG (rat)	GATA4 (rabbit)	CDX2 (mouse)	Donkey rat (488)	Donkey rabit (555)	Donkey mouse (647)

3.5 Confocal microscopy

Following fixation and fluorescent immuno-staining, embryos were transferred on glass-bottomed culture plates and placed on the stage of an inverted FV10i Confocal Laser Scanning Microscope, which included FV10i-SW image acquisition software (Olympus®). Embryos were imaged in a series of z-stacks with step-size of 1.5 or 2µm (for example, an approximately 100µm diameter spherical blastocyst embryo at E4.5 will be imaged in 50 stacks, or 30µm diameter ICM at E4.5 (step size 1.5) will be imaged in 20 stacks). Embryo images (including individual z-stacks and projections) were analysed using FV10-ASW 4.2 Viewer software (Olympus®).

3.6 Cell number quantification (in blastocysts and isolated ICMs) and statistical analysis

The total number of cells (per blastocyst/isolated ICM) were counted based on pan-nuclear DAPI staining of all embryonic cells. In experiments to visualize both TE and ICM lineages, inner cells were divided into two groups based on detectable and sole NANOG/SOX2 or GATA4 IF (denoting respective, EPI and PrE lineages), and the trophectoderm lineage as based on detectable CDX2 IF. In those experiments, were NANOG/SOX2 and GATA4 were assayed (without a TE marker), cells that did not stain for either GATA4 or NANOG/SOX2, were classified as outer/TE cells (also based on their relative spatial outer-position). Counting of the total number of cells in each category was carried out manually using ImageJ (Fiji) software and data accumulation/record using Microsoft Excel; with the use of GraphPad Prism for further statistical analysis and chart preparation.

3.7 Blastocyst size and volume calculations

The volume of blastocyst cavities was calculated by measuring their inner circumference, whereas the volume of the whole embryo, was calculated by measuring the outer circumference of the entire blastocyst; both employing the centrally located widest/equatorial z-slice image, using Fiji (ImageJ) software. The settings used in the Fiji program were as follows: Analyse>Set Measurements; with the "Perimeter" option selected, the "Polygon selection" tool was used mark the required circumferences. The radii of the measured circumferences were mathematically derived and used to calculate an approximate volume for all embryos analysed. The calculated volume in picolitres (pL) was plotted as a scatter-graph, representing the complete assayed embryo population, with mean and standard deviations (SD) indicated.

3.8 Statistical analysis

Statistical analysis was carried out using GraphPad Prism. The specific statistical tests used were determined by tests for Gaussian distribution of the respective dataset. Datasets with normal distribution were compared by using unpaired two-tailed t-test and datasets with log-normal distribution were compared using Mann-Whitney tests (specified within respective data analysis figure legends). Respective p-values arising from the statistical tests are plotted within the graphs and the degree of significance determined as described (Table 3):

Tab. 3: Degree of Significance:

P value	Wording	Summary
< 0.0001	Extremely significant	****
0.0001 to 0.001	Extremely significant	***
0.001 to 0.01	Very significant	**
0.01 to 0.05	Significant	*
≥ 0.05	Not Significant	ns

4 Results

4.1 Learning Immunosurgery: ICM isolation technique

To further investigate the role of p38-MAPK in relation to PrE differentiation defects, not only on blastocysts but also on isolated ICMs, a new technique had to be introduced to the laboratory; one enabling large numbers of ICMs to be prepared in a short period of time (Wigger et al., 2017). Blastocysts at the E3.5 stage (92-96 hours post hCG injection – relating to the super-ovulation process) consists of both ICM and TE cells and it is difficult to remove TE layer and leave an intact ICM by microsurgical procedures, since it can damage some cells of the ICM. An alternative isolation technique is called immunosurgery (IS) and makes use of antibodies that bind to the outer trophectodermal cells but not to the cells of the inner cell mass. After exposure of the embryo to complement factors (a mixture of proteins that are part of the immune system) the cells that have bound antibodies are destroyed, as the complement attaches to the antibodies and initiates cell lysis, leaving the intact inner cell mass that can be subsequently be cultured (Handyside & Barton, 1977). When isolated ICMs are cultured for a further 24 hours after IS (*i.e.* the equivalent E3.5-E4.5 blastocyst maturation window), an outer PrE layer encapsulating a deep specified EPI is formed. The progress of immunosurgery can be seen in Figure 5.

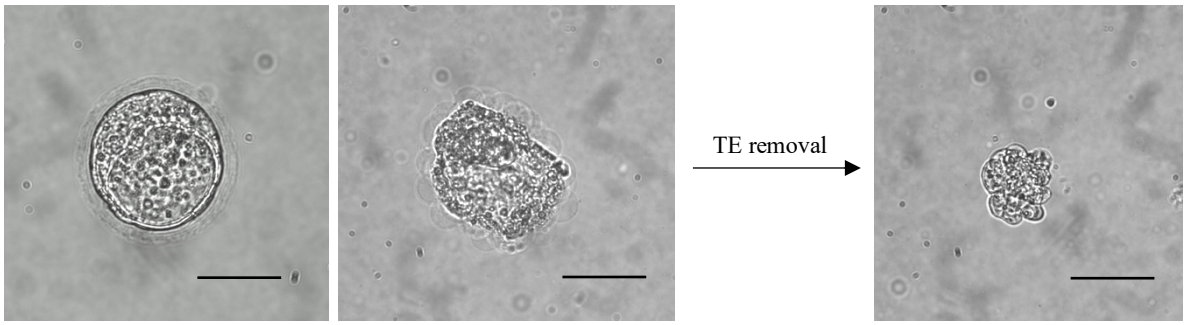

Figure 5: Representative live microscopy images of the IS technique. The first image on the left shows an intact E3.5 blastocyst before removing the *zona pellucida.* The second image, in the middle, shows the blastocyst after incubation in mouse serum and then after incubation in complement; note the ICM with lysed surrounding TE cells. The third image (on the right) shows the isolated ICM after removal of lysed TE cells by pipetting through a narrow-gauge glass pipette; scale bar represents 30µm.

To confirm that IS was performed correctly, ICMs were immuno-fluorescently (IF) stained for CDX2 (a marker of the TE lineage), NANOG (an early pan ICM and later EPI specific EPI marker) and GATA4 (a marker of specified and differentiating PrE). The total number of GATA4, NANOG and CDX2 positive cells in each isolated ICM, which were either fixed

immediately after IS or fixed after 24 hours of *in vitro* culture, was determined from acquired confocal microscopy z-section series of entire ICMs. In Figure 6 (ICMs at stage E3.5 and, after 24 hours of *in vitro* culture, at the equivalent E4.5 stage) it can be observed that there are no GATA4+ nor CDX2+ cells in freshly isolated ICMs; indicating PrE differentiation had not been initiated (as would be expected at the E3.5 time-point) and all TE cells were successfully removed. Alternatively, expressed, that the IS procedure was successfully executed (Figure 7 provides exemplar E3.5 ICM confocal micrograph z-section projections, stained for NANOG and GATA4). In Figure 6, similar data representing isolated ICMs cultured to the E4.5 stage is shown, *i.e.* E3.5 stage IS isolated ICMs that were cultured in KSOM+AA and fixed after 24 hours. These data confirm that a GATA4+ PrE mono-layer of cells appropriately formed around a NANOG+ and encapsulated EPI, rather than a CDX2+ TE mono-layer that would have formed if the initial blastocyst IS had been performed too early (*i.e.* prior to the known point of irreversible TE cell-fate commitment (Posfai et al., 2017; Wigger et al., 2017). These latter results are further confirmation that the employed IS was successfully performed (Figure 8 provides exemplar E4.5 ICM confocal micrograph z-section projections, IF stained in this case for SOX2, as an alternative EPI marker, and GATA4).

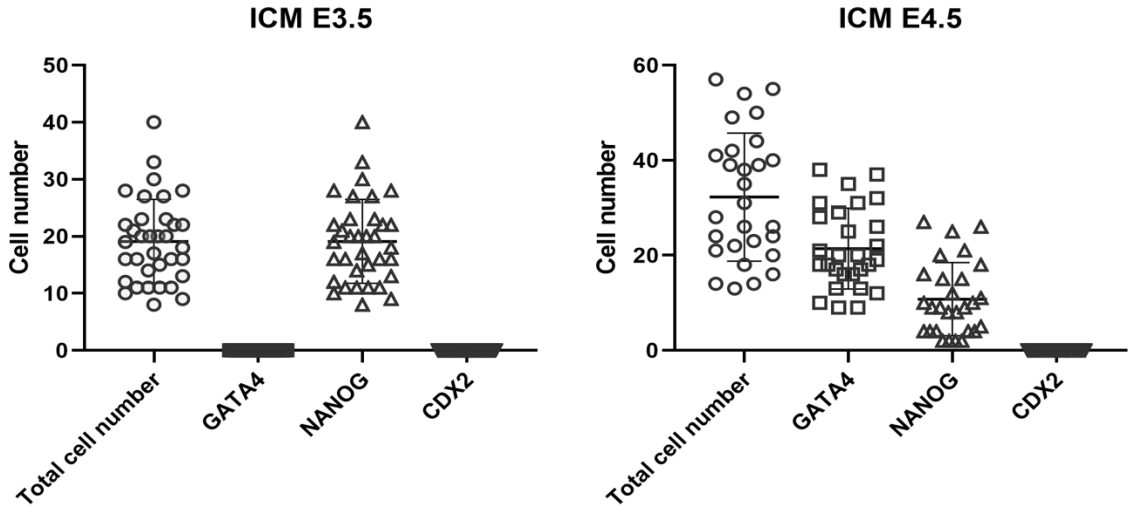

Figure 6: Graph detailing total, GATA4+, NANOG+ and CDX2+ cells of isolated ICM at stage E3.5 (fixed immediately after IS) and E4.5 stage (fixed 24 hours after IS). Errors are represented as standard deviations.

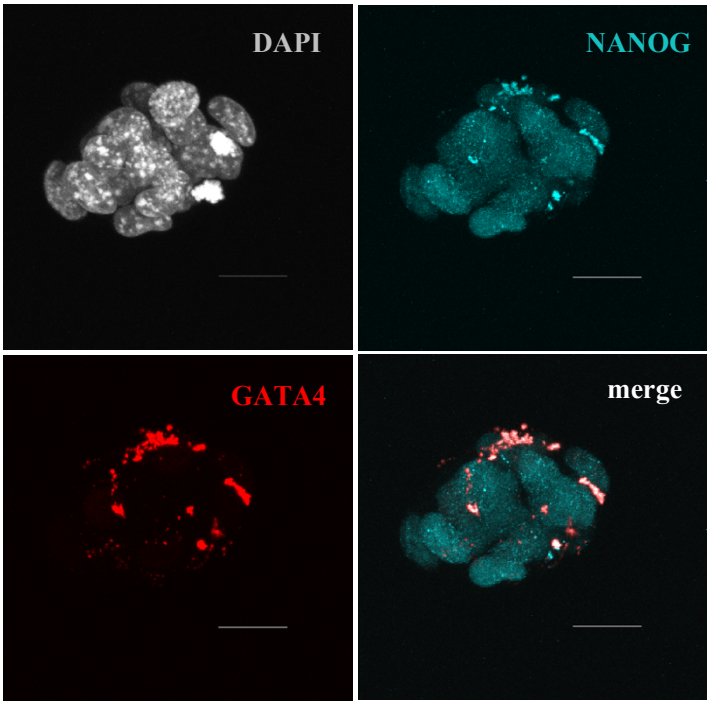

Figure 7: Representative projected z-stack confocal images of ICMs fixed immediately after IS and IF for EPI marker NANOG (blue) and PrE marker GATA4 (red) at E3.5. For comparison, DNA DAPI counterstain (grey) is shown in the image in the left upper corner and a merged NANOG and GATA4 channel image in the lower right corner; scale bar represents 10μm.

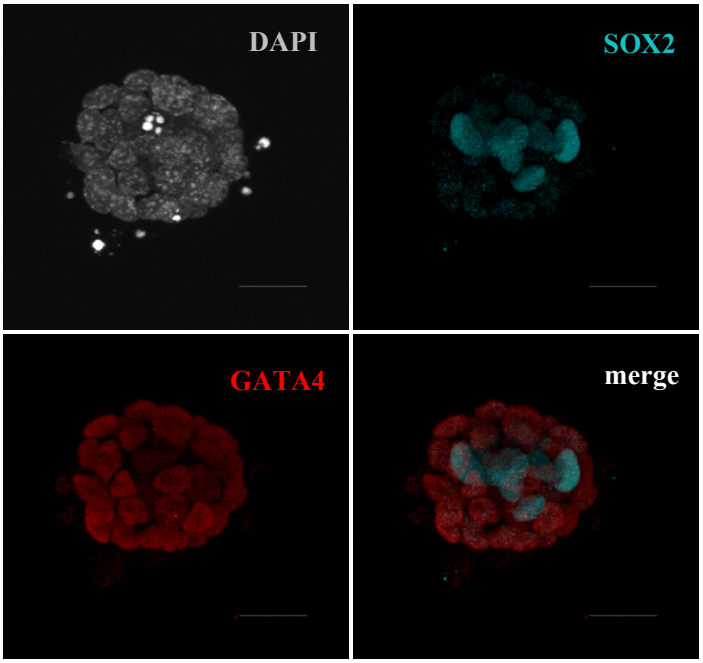

Figure 8: Representative projected z-stack confocal images of IS isolated ICMs fixed after 24 hours of post-IS *in vitro* culture and IF stained for EPI marker SOX2 (blue) and PrE marker GATA4 (red) at the equivalent E4.5 stage. DNA DAPI counterstain (grey) is shown in image in the upper left corner and a merged SOX2 and GATA4 channel image in the lower right corner; scale bar represents 10μm.

4.2 Isolated early ICMs are able to recreate the TE epithelial layer

IS isolated early ICM cells, that are TE-deprived (and those ICM cells of intact early blastocysts), are able to sustain their totipotency (*i.e.* an ability to differentiate into all primary cell lineages) but soon lose the ability to give rise to TE (during the early, equivalent, 32-cell blastocyst stage) (Posfai et al., 2017; Wigger et al., 2017). The FGF/MAPK signalling pathway is a regulator of totipotency; once the specification of PrE and EPI precursor cells (dictated by FGF/MAPK signalling) within the ICM is established (and TE fate has become irreversibly committed) (Posfai et al., 2017), isolated ICMs can form only PrE layer on their surface. However, it should be noted that individual ICM cells maintain their ability to switch between PrE and EPI fate for a substantially longer time (around E4.25) (Yamanaka et al., 2010). Indeed in ICMs isolated from E3.5 embryos, the ultimate PrE layer can originate from both potential EPI and PrE precursors, but in ICMs isolated from E4.5, such plasticity is reduced and the PrE layer is formed mainly by proliferating PrE cells, originally presented on the surface of the ICM (an rarely by EPI cells switching their fate) (Wigger et al., 2017).

Therefore, we wanted to confirm, that the cells of ICM isolated from early (E3.0-E3.5) freshly flushed blastocysts (*i.e.* not *in vitro* cultured), are still totipotent and therefore can reconstruct the TE layer, as was assayed in Wigger at al., 2017. Mouse blastocysts taken after 89-91 hours post-hCG injection were subject to IS, and *in vitro* cultured in KSOM+AA media for 24 hours, fixed and assayed for lineage marker protein expression by confocal microscopy based IF. As expected, recreation of the TE layer was observed and thus a higher number of CDX2+ cells were recorded (Figure 9) than in ICMs, also assayed at E4.5 but isolated later (also fixed 24 hours after *in vitro* culture as detailed in Figure 6). The results indicate, that when IS under these conditions is performed, it is too soon to create a complete PrE layer, *i.e.* corresponding to a point before the second cell fate decision is initiated (or the first is complete), and the isolated ICM cells retain the totipotency necessary to recreate a TE fate. Further, in some cases, where the TE layer forms, isolated ICMs are able to reform a whole blastocyst (*i.e.* reform a blastocyst cavity). Collectively, these data inform the precise (and earliest) timings at which IS isolation, and *in vitro* culturing, of ICMs can reliably recreate an outer TE or PrE epithelial mono-layer.

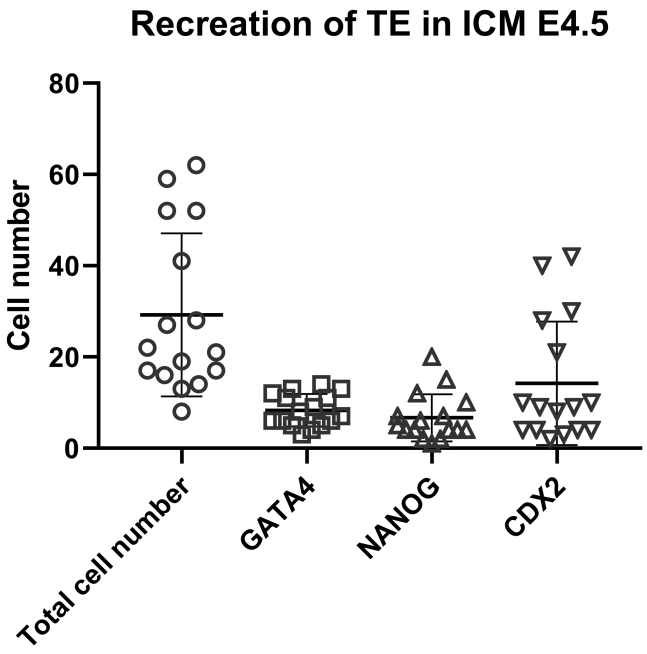

Figure 9: Graph showing total cell number, GATA4+, NANOG+ and CDX2+ cells of ICMs isolated at 89-91 hours post-hCG and i*n vitro* cultured to the E4.5 stage (fixed 24 hours after IS). Errors are represented as standard deviations.

4.3 Confirmational p38-MAPKi in intact blastocysts between E3.5 and E4.5

As a control and verification of the p38-MAPK inhibitor (SB220025) regime, we repeated the inhibition of p38-MAPK using intact blastocysts. This was to ensure we observed the same specific p38-MAPK inhibition induced deficit in PrE differentiation (without affecting specification of the EPI) as we previously reported (Bora et al., 2019, 2020, 2021; Thamodaran & Bruce, 2016). We wanted to prove that the phenotype of p38-MAPKi is consistent and that we will be able to rely on the inhibitor for the IS isolated ICMs experiment. Accordingly, E3.5 stage mouse embryos/blastocysts were cultured under both control (+DMSO) and p38-MAPK inhibited (+SB220025 - 20μM) conditions until the late blastocyst stage (E4.5). Embryos were then fixed and IF stained for NANOG (EPI), GATA4 (PrE) and CDX2 (TE) protein expression and subsequent complete confocal microscopy z-series sections acquired, per embryo. The average total, inner and outer cell number per group, plus the number of NANOG and GATA4 expressing ICM cells and CDX2 positive TE cells counted; and the average blastocyst cavity volume calculated. These confirmatory results are summarised in Figures 10-15.

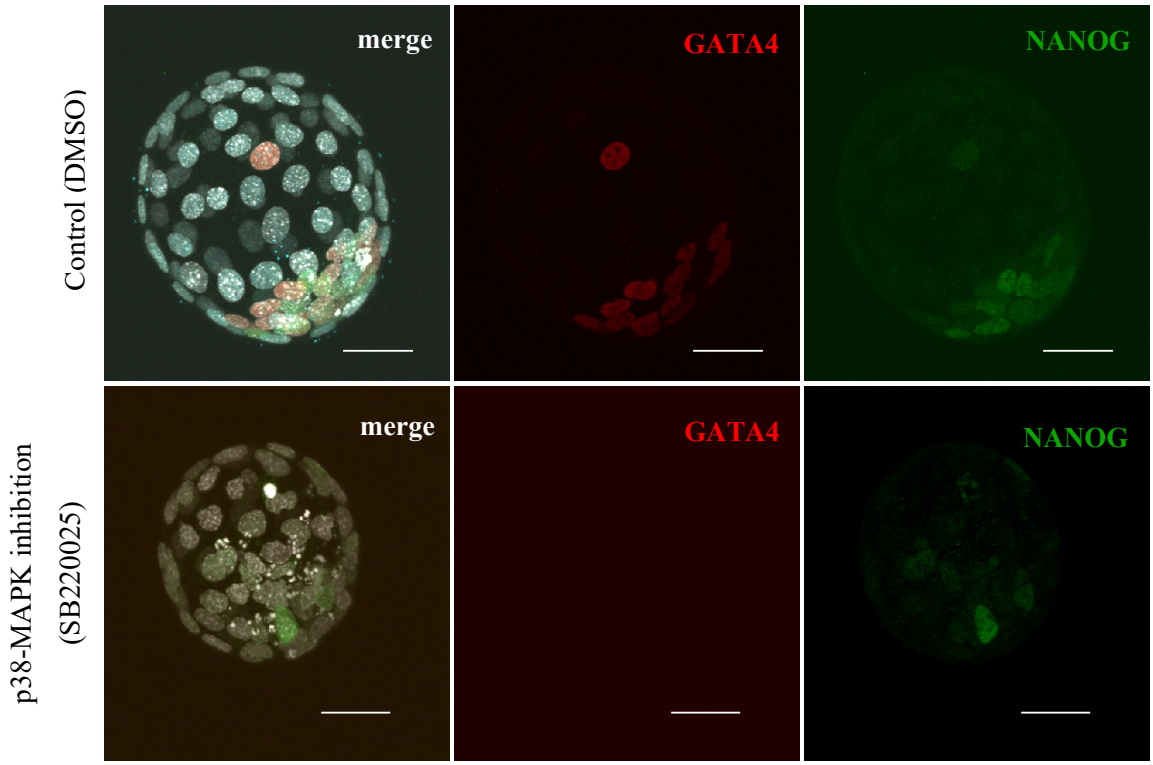

Figure 10: Representative projected z-stack confocal images of blastocysts treated (between E3.5-E4.5) with DMSO control (upper row) or SB220025 p38-MAPK inhibitor (lower row), fixed and IF stained for EPI marker NANOG (green) and PrE marker GATA4 (magenta) at E4.5. DNA DAPI counterstain (grey) is shown in merged image; scale bar represents 20μm.

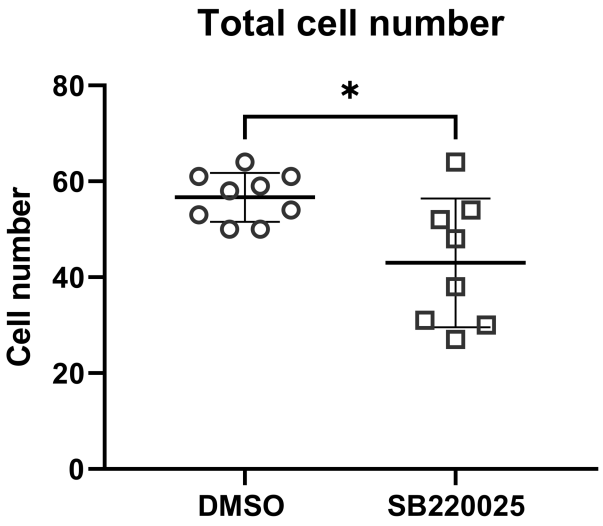

Figure 11: Graph showing comparison between total cell number of control treated blastocysts (DMSO) and inhibited blastocysts (SB220025); E3.5-E4.5. Errors represent standard deviations and statistical unpaired t-test was used; p-value indicated * (0.0124).

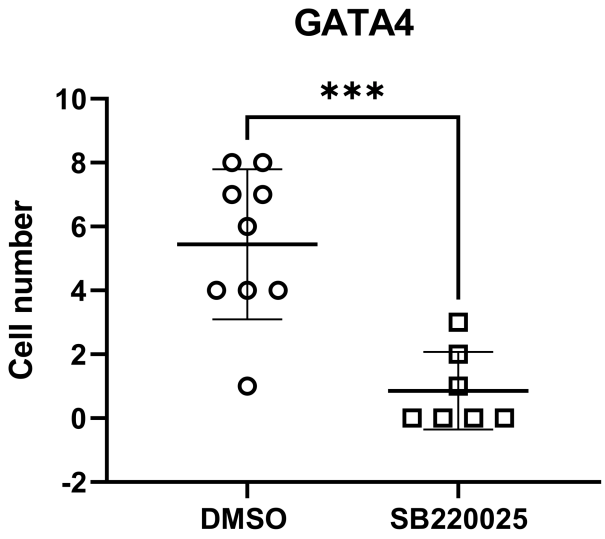

Figure 12: Graph showing cell number of GATA4 positive cells of control treated blastocysts (DMSO) and inhibited blastocysts (SB220025); E3.5-E4.5. Errors represent standard deviations and statistical Mann-Whitney test was used; p-value indicated *** (0.0006).

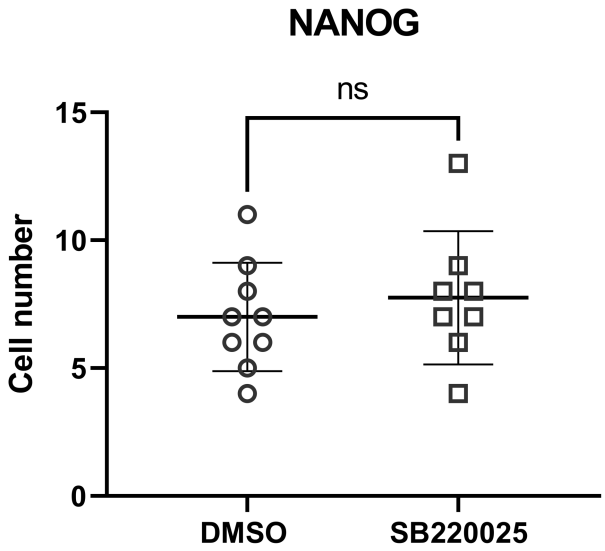

Figure 13: Graph showing cell number of NANOG positive cells of control treated blastocysts (DMSO) and inhibited blastocysts (SB220025) at E4.5 stage. Errors are presented as standard deviations and statistical unpaired t-test was used; p-value stated ns (0.5229).

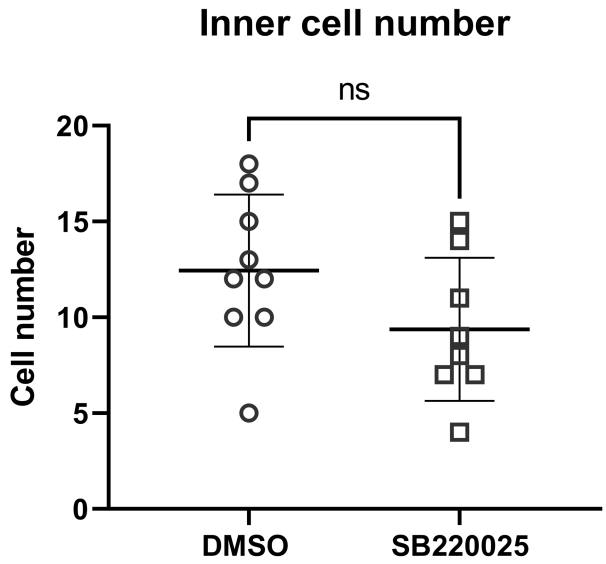

Figure 14: Graph showing comparison of inner cells number of control treated blastocysts (DMSO) and inhibited blastocysts (SB220025) at E4.5 stage. Errors are presented as standard deviations and statistical unpaired t-test was used; p-value stated ns (0.1230).

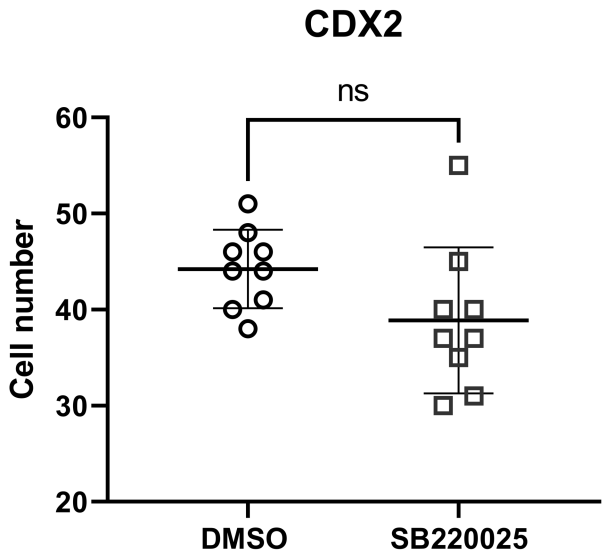

Figure 15: Graph showing cell number of CDX2 positive cells of control treated blastocysts (DMSO) and inhibited blastocysts (SB220025) at E4.5 stage. Errors are presented as standard deviations and statistical unpaired t-test was used; p-value stated ns (0.0824).

As can be seen in Figure 10, detailing representative micrographs showing confocal images of blastocysts treated (between E3.5-E4.5) with DMSO control (upper row) or SB220025 p38-MAPKi, p-38-MAPK inhibition was associated with reduced GATA4 expressing ICM cells and continued expression of NANOG. These data confirm that the employed p38-MAPKi inhibition regime recapitulated our previously reported block in PrE specification and differentiation (Bora et al., 2019; Thamodaran & Bruce, 2016). This result was also supported by cell counting analyses in Figures 11-15. As can be seen in Figure 11, there was a reduced number of cells in total (from 57±3 to 41±7); this effect is consistent with previous data (Bora et al., 2021; Thamodaran & Bruce, 2016). Importantly, the number of GATA4 expressing ICM cells was consistently, significantly and markedly reduced (from 5±2 to 0.1±1) under p38-MAPKi conditions (Figure 12); confirming impaired PrE specification/differentiation. In Figure 13, we also observed a consistent lack of statistically significant differences in number of NANOG+ ICM cells in p38-MAPK inhibited blastocyst vs. control treated blastocysts (DMSO); from 11±3 versus 10±2, respectively. As can be observed in Figure 14, the number of inner cells was slightly reduced (from 13±2 to 9±2) but not significantly. In Figure 15, we counted and compared number of outer CDX2 positive cells in control and SB220025 p38-MAPKi blastocysts and there was also no significant difference (from 45±2 to 40±2), suggesting the p38-MAPK inhibitor (SB220025) was not cytotoxic.

We next measured the average blastocyst cavity volumes (pL) in the control (DMSO) and p38-MAPK inhibitor treated blastocysts (Figure 16). We found that as predicted, p38-MAPK inhibited blastocysts presented with significantly reduced cavity volumes (from 1079pL in controls to 808pL in p38-MAPKi embryos – Figure 16). Therefore the used p38-MAPKi conditions are associated with reduced blastocyst cavity expansion, as previously described (Bora et al., 2019; Thamodaran & Bruce, 2016). In conclusion all assayed data on p38-MAPKi of blastocysts are consistent with our previous reported studies (Bora et al., 2019; Thamodaran & Bruce, 2016) and therefore we proved the phenotype of p38-MAPKi is consistent and that we can apply this inhibitor to the planned experimentation on IS isolated ICMs.

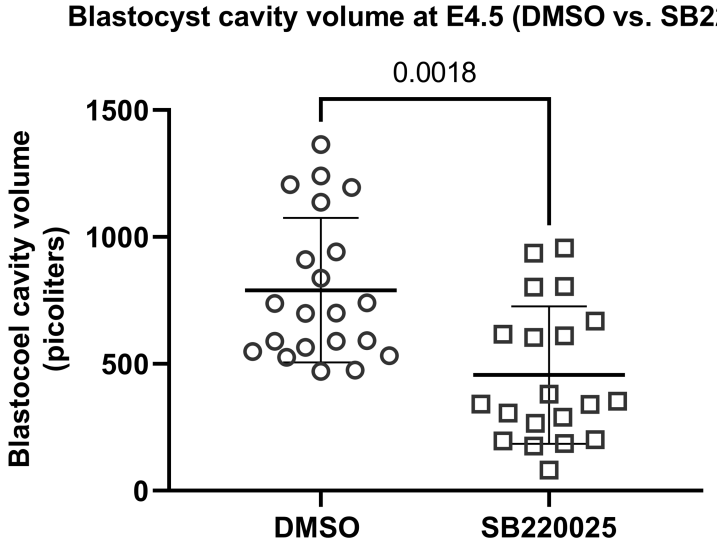

Figure 16: Mean blastocyst cavity volumes (pL) of E4.5 stage blastocysts treated with control DMSO (n=21) or p38-MAPK inhibitor SB220025, from E3.5-E4.5 (n=20). Errors are presented as standard deviations and statistical Mann-Whitney test was used; p-value indicated ** (0.0018).

4.4 p38-MAPK inhibition in IS isolated and *in vitro* cultured ICMs, results in PrE cell-fate defects

As described above (chapter 1.4.1), the p38-MAPK pathway is reported to be necessary between E3.5 to E4.5 for appropriate PrE specification/differentiation in the mouse blastocyst. Chemical inhibition of p38-MAPK during this developmental window severely impairs PrE specification and differentiation (manifest as robustly reduced average numbers of GATA4+ cells per ICM,) as well as cavity expansion (Bora et al., 2019, 2020, 2021; Thamodaran & Bruce, 2016). A report by Ryan et al., 2019, showed chemical and mechanical impairment of blastocyst cavity size during early blastocyst maturation (E3.5-E4.0) results in reduced levels of PrE specific marker protein expression (*i.e.* GATA4 – as assayed at E4.0); a result resonating with that describing fewer PrE cells after p38-MAPK inhibition between E3.5-E4.5 (Bora et al., 2019; Thamodaran & Bruce, 2016). Therefore, we wanted to test whether the p38-MAPKi PrE differentiation phenotype is mediated by a TE defect, leading to smaller cavity size, or if it is an ICM autonomous effect. In testing this hypothesis, the inhibition of p38-MAPK had to be performed exclusively on ICMs. (*i.e.* in the absence of a TE and a blastocyst cavity).

To achieve the experimental aim, we decided to use ICMs isolated from blastocysts cultured from embryos collected at the 8-cell stage, rather than freshly flushed blastocysts. This was to

provide a finer degree of experimental control, as the timing for immunosurgery and the p38-MAPKi sensitive window are very precise, and freshly flushed blastocysts are known for their heterogeneity (Rosàs-canyelles et al., 2020), compared to *in vitro* cultured embryos. Indeed, we empirically found it was important to perform this experiment in a precise time sensitive window and that culturing blastocyst from 8-cell stage did indeed offer more control and higher number of blastocysts at same stage were obtained for simultaneous IS.

In previously described experiments (Bora et al., 2019, 2020; Thamodaran & Bruce, 2016) employing specific pharmacological 'inhibition and release'-based experimental regimes (using the compound SB220025), a minimal time window of p38-MAPKi required for eliciting blastocyst PrE differentiation phenotypes of E3.5 +7 hours was determined. However, the preferable timing, resulting in maximal phenotypes, was determined as E3.5 +24 hours of p38-MAPKi. However, because IS isolated ICMs are much smaller in size (around 25μm) than E3.5 stage blastocysts (also lacking a ZP, an epithelised TE and cavity), it was decided to reduce the timing of inhibition from 24 hours to 12 hours. We also titrated the concentration of the SB220025 inhibitor used for this experiment on ICMs between a 20μM concentration (confirmed concentration used for E3.5 blastocysts inhibition), through a 10μM concentration to a 5μM concentration. Based on cell death, the 10μM and 20μM concentration of inhibitor was determined to be cell toxic. Therefore, we determined that a 5μM concentration of inhibitor was the most eligible concentration for this experiment. Thus, E3.5 stage mouse ICMs were cultured immediately after IS under both control (+DMSO) and p38-MAPK inhibited (+SB220025 - 5μM) conditions for 12 hours. After 12-hour inhibition, the ICMs of both conditions were transferred into regular KSOM+AA media and further cultured for another 12 hours. ICMs were then fixed and IF stained for NANOG and GATA4 protein expression and a complete z-series of confocal sections per ICM acquired. The average total cell number per group and the number of NANOG and GATA4 expressing cells was then counted. Figure 17 provides a descriptive scheme of this experiment and Figure 18 shows representative micrographs of ICMs from the control/DMSO and p38-MAPKi/SB22025 treated groups.

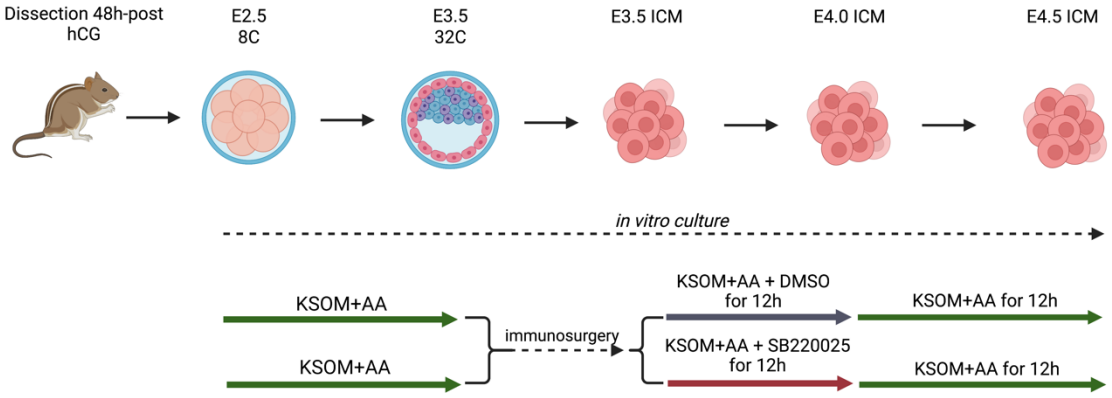

Figure 17: Descriptive scheme of p38-MAPK inhibition (p38-MAPKi) experiment on IS isolated ICMs; blastocysts were cultured from the 8-cell stage; ICMs were then cultured after IS in both conditions (SB220025 inhibitor of p38-MAPK and DMSO as a control) for 12 hours and then transferred into regular KSOM+AA media and cultured for another 12 hours before fixing and confocal IF; the scheme was created using online web application BioRender.

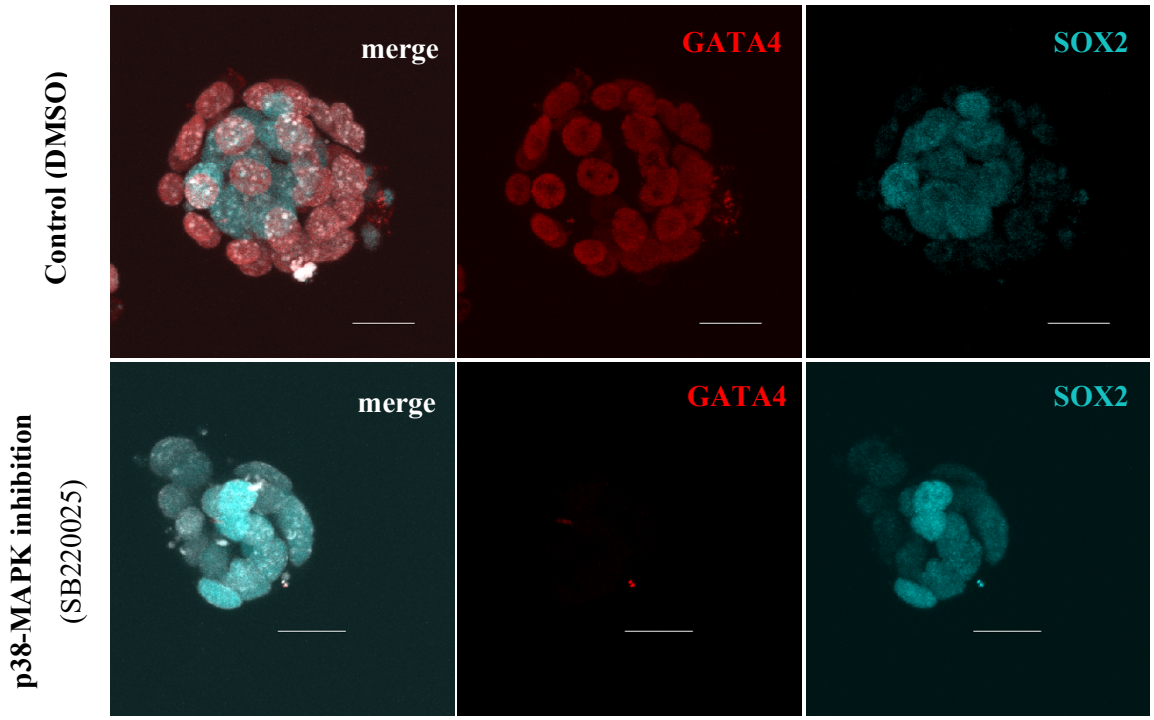

Figure 18: Representative projected z-stack confocal images of IS isolated ICMs (92-96hours post hCG injection) treated with DMSO control (upper row) or SB220025 p38-MAPK inhibitor (lower row), for 12 hours and then cultured for a further 12 hours in regular KSOM+AA media, fixed and IF stained for the EPI marker SOX2, (blue) and PrE marker GATA4 (red) at E4.5. DNA DAPI counterstain (grey) is shown in merged image; scale bar represents 10μm.

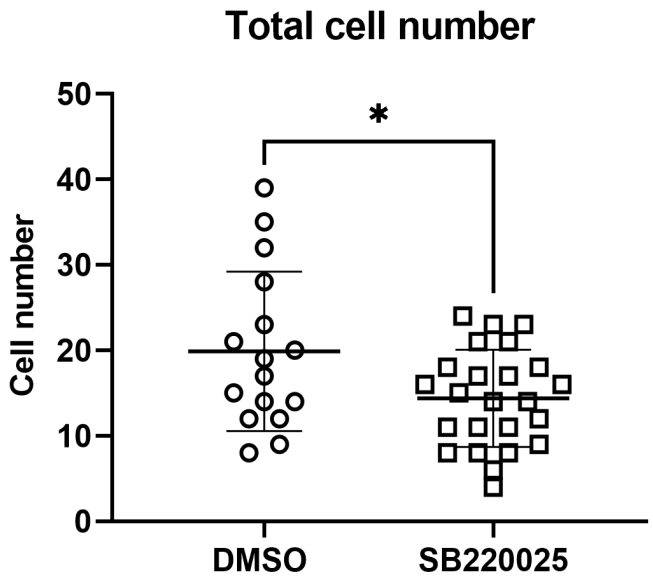

Figure 19: Graph showing a comparison between total cell number of control treated ICMs (DMSO) and inhibited ICMs (SB220025). Errors are presented as standard deviations and statistical un-paired t-test was used; p-value indicated * (0.0257).

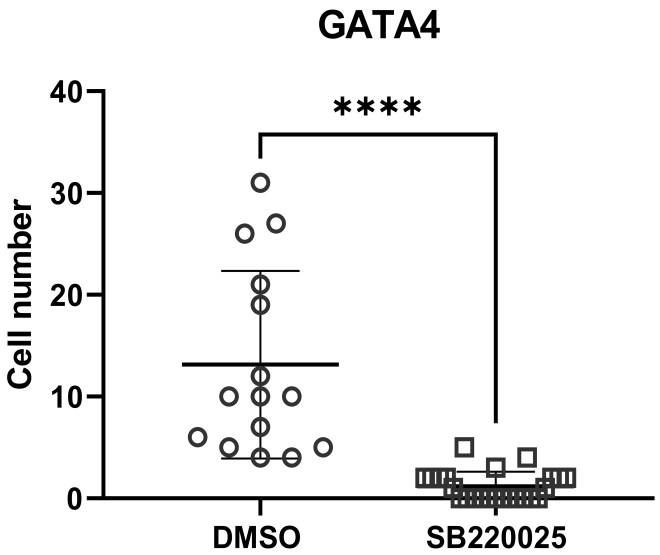

Figure 20: Graph showing cell number of GATA4 positive PrE cells of control treated ICMs (DMSO) and inhibited ICMs (SB220025). Errors are represented as standard deviations and statistical Mann-Whitney test was used; p-value indicated **** (<0.005).

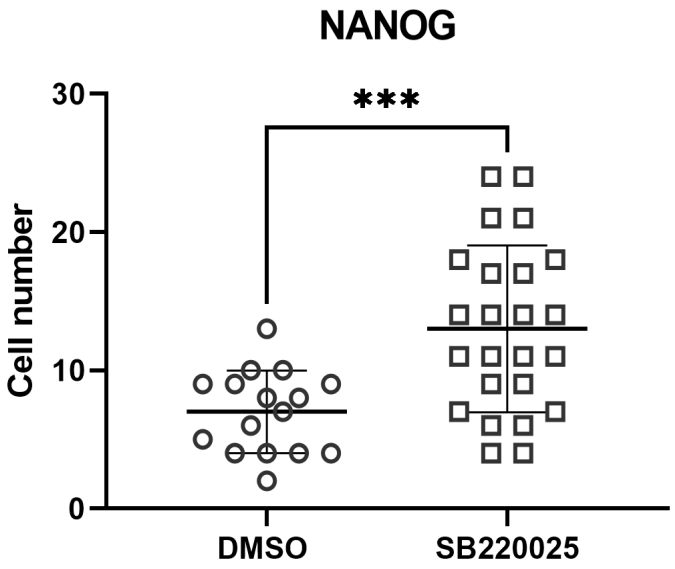

Figure 21: Graph showing cell number of NANOG positive cells of control treated ICM (DMSO) and inhibited ICMs (SB220025). Errors represent standard deviations and statistical un-paired t-test was used; p-value indicated *** (0.0026).

In Figure 19, the total number of cells between the control and p38-MAPKi group of ICMs was compared and the data showed that there was a small, but significant, reduction in total ICM cell number after p38-MAPKi (from 20±5 to 14±3); agreeing with previous intact blastocyst derived ICM data (Figure 12); however not small enough to account for the observed reduction in GATA4 expressing PrE cells (Bora et al., 2021; Thamodaran & Bruce, 2016). Indeed, as can be seen in Figure 20, the number of ICM cells expressing GATA4 (indicating PrE differentiation) was significantly reduced, from 13±4 to 0±2. Furthermore the number of ICM cells expressing NANOG (Figure 21) (indicative of either EPI specification or potentially uncommitted ICM cells) was increased (from 7±2 to 14±3); again agreeing with previous reports of similarly treated intact blastocysts (Bora et al., 2019; Thamodaran & Bruce, 2016); where such an increase was revealed (via NANOG and GATA6 specific IF staining) to reflect normal levels of EPI specification (marked by sole NANOG expression) and increased numbers of uncommitted ICM cells (co-expressing NANOG and GATA6; at the expense of PrE differentiation). Although, we have to consider the fact, that we used a smaller concentration of p38-MAPK inhibitor (5μM) on isolated ICMs and therefore the effect might be slightly different from was reported in Bora et al., 2021, 2019 and Thamodaran & Bruce, 2016; *i.e*. in the present experiments, the lower concentration of inhibitor may increase number of uncommitted/potential PrE progenitor cells rather than result in their cell death (that

when assayed by NANOG IF are indistinguishable from EPI specified cells – hence increasing the number of NANOG expressing cells observed under p38-MAPKi conditions; nevertheless the main result of significant and robust impairment of PrE specification is consistent with intact blastocyst data and is the main conclusion of these experiments. Collectively, these data derived from studies on isolated ICMs, confirm that the p38-MAPK inhibition regime historically employed in intact blastocysts, solely during ICM maturation (E3.5-E4.5), was effective at impairing PrE formation via a mechanism that is more likely to be ICM specific/autonomous rather than other mechanisms related to impaired TE function and/or blastocyst cavity expansion.

5 Disscusion

The first aim of this thesis project was to learn immunosurgery, a technique that would enable the collection of large numbers of isolated ICMs, that could be used to test the hypothesis that p38-MAPKi induced defective PrE specification/differentiation phenotypes are mediated in an ICM specific/autonomous manner.

Immunosurgery is a very effective method of removing blastocyst TE cells to obtain an isolated ICM. Cells of the TE are destroyed by brief exposure to mouse antibodies, coating their surface, in tandem with complement activity (antibody-dependent complement, leading to a cascade ending in cell lysis). Therefore, this protocol works on embryos with an intact trophectoderm; whilst the structural integrity of the blastocyst protects the ICM from the immunologically induced cell lysis reaction (the reaction itself occurring on the TE surface of the blastocyst) (Goldberg & Ackerman, 2020). According to Wigger et al. 2017, ICMs isolated by IS at E3.0 can reconstruct the TE epithelial layer and form a blastocyst cavity. In this thesis, we confirmed that IS performed sooner then 92 hours post hCG (late E3.0 and early E3.5 blastocysts) is permissive for the ICM cells to reconstruct a TE layer, and even reform the whole blastocyst (characterised by a reformed cavity). We also wanted to confirm, that ICMs isolated by IS at later E3.5 stages form an outer PrE layer rather than a regenerated TE layer, as was also described in Wigger et al., 2017. In chapter 4.2, we have recapitulated the experiment and obtained the same results, indicating that IS performed 92-96 hours post hCG allows ICM cells to form only an outer PrE layer on the surface of the ICM with EPI cells encapsulated inside (*i.e.* surrounded by GATA4+ PrE cells) (Figure 14).

In a previous paper, our group identified a functional role of p38-MAPK during preimplantation mouse embryo development; specifically as a required activity to allow PrE specification, and subsequent differentiation, during early mouse blastocyst maturation (Bora et al., 2019, 2020; Thamodaran & Bruce, 2016). As a control and a prelude to experiments on IS isolated ICMs, we recapitulated these p38-MAPKi-assoiated findings, showing reduced numbers of GATA4 expressing PrE cells (Figure 12); moreover, we also verified, that p38-MAPKi blastocyst (E3.5-E4.5) had statistically significant smaller cavities (Figure 16), as was described in Bora et al., 2021. Thus, it was proved, that the phenotype of p38-MAPKi was consistent and provided confidence, that we could rely on the inhibitor for the IS isolated ICMs experiments. In a paper by Ryan et al. 2019, it was reported that there is positive correlation between expanding blastocyst cavity size/volume and appropriate ICM lineage specification (assayed by ICM cell lineage marker protein expression levels) and segregation, particularly

effecting the PrE. We connected these findings with the fact, that p38-MAPKi in intact blastocysts (E3.5-E4.5) is also associated with smaller cavity size, and thus hypothesised if the p38-MAPKi induced PrE deficient phenotypes we had previous reported (Bora et al., 2019, 2021; Thamodaran & Bruce, 2016), had its origin in the regulation of the expanding blastocyst cavity. Alternatively expressed, our hypothesis was, p38-MAPKi PrE differentiation induced phenotypes maybe mediated by a TE defect, affecting cavity size/volume expansion, rather than being ICM autonomous/specific. Therefore, after perfecting the IS technique, we exposed isolated ICMs to p38-MAPKi to test our hypothesis as a part of the second aim of this thesis. The results clearly indicated that ICMs cultured in KSOM+AA plus p38-MAPKi for 12 hours had a robust and statistically significant lower number of GATA+ PrE cells (and lower number of cells in total; yet certainly not enough to account for the observed PrE phenotype). These results confirm that p38-MAPKi has the same effect on IS isolated ICMs lacking a TE layer and a cavity, as in intact maturing blastocysts; a reduction in the number of GATA4+ PrE cells. The results also demonstrated, that p38-MAPKi ICMs had more NANOG positive cells; indicating EPI specification is most likely not affected (as we reported in intact blastocysts, Figure 13) (Bora et al., 2021; Thamodaran & Bruce, 2016) and that the extra NANOG positive ICM cells are most likely to be uncommitted cells (as seen in the blastocyst); that could possibly be assayed (and will be assayed in the future) using a combination of GATA6/NANOG (or SOX2) IF marker staining. We speculate, that the effect of the employed concentration of p38-MAPK inhibitor on isolated ICMs, that is smaller than on blastocysts (5μM versus 20μM), might account for the slightly different data in regard to the comparative number of NANOG expressing cells (not GATA4 expressing cells) between control and p38-MAPKi treated intact blastocysts and ICMs (Bora et al., 2021 and Thamodaran & Bruce, 2016); where the number of NANOG positive slights were slightly increased or remained statistically equal after p38-MAPKi in intact blastocysts. As stated above, this most likely reflects an increased population of uncommitted and failing PrE progenitors in ICMs and indicate a greater degree of cell death of the same population in intact blastocysts; nevertheless, the evidence suggests that in both cases PrE specification/differentiation is impaired and EPI specification is unaffected. Further, we observed that isolated ICMs that recreated a TE and cavity (after 12 hours of inhibition) were also affected by p38-MAPKi, as we observed a PrE (GATA4+) deficit in the ICM cells of such reforming blastocysts (*data not shown*; due to low n-numbers; we can speculate that this suggests a development "reset" in isolated ICMs, that pushes the p38-MAPKi PrE sensitive window temporally back).

Furthermore, the combined data indicate that p38-MAPKi induced PrE specification/differentiation defective phenotype is indeed an ICM autonomous effect and not significantly contributed to by TE-related biology and blastocyst cavity expansion. Indeed, recent work from our group indicated there are strong ICM PrE progenitor cell autonomous effects, related to temporally discreet regulation of translation, which are supported by findings of this thesis. Thus, the general acquired knowledge supports a model by which the PrE progenitors of the early mouse blastocyst ICM respond to some, as of yet unknown stimulus (that is not likely to be FGF4-FGFR1/2 related – Bora et al., 2021), that stimulates p38-MAPK activity, permitting their priming for PrE specification and subsequent differentiation, via a mechanism involving regulated protein translation. With the confirmation of p38-MAPKi deficient PrE phenotypes in IS isolated ICMs, the possibility of repeating some biochemical analyses of the (phospho-) proteome and transcriptome that was previously performed on intact blastocysts (Bora et al., 2021) is a real possibility; this would be an advantage as p38-MAPKi related changes that are specific for the TE would be filtered out, allowing a more focus investigation of p38-MAPKs role within ICM cell-fate specification (although this would require careful coordination to derive enough IS isolated ICM material, with particular reference to (phospho-)proteomic and transcriptomic studies).

6 Conclusion

We have previously confirmed that p38-MAPKi is associated with ICM cell-fate defects, specifically effecting PrE specification and differentiation (but not EPI specification), and impaired blastocyst cavity expansion (Bora et al., 2020; Thamodaran & Bruce, 2016). Here, we have again confirmed the effect of p38-MAPKi on PrE differentiation in intact blastocysts and we have also expanded the knowledge of p38-MAPKi, solely using IS isolated ICMs (a newly introduced and established technique for our laboratory, required for this thesis project and future investigations). We have confirmed p38-MAPKi PrE deficient phenotypes are not appreciably contributed to by TE/blastocyst cavity defects but are ICM specific and autonomous. Work described within this thesis contribute a significant component of a manuscript currently under preparation.

References

Bell, C. E., & Watson, A. J. (2013). p38 MAPK Regulates Cavitation and Tight Junction Function in the Mouse Blastocyst. *PLoS ONE*, *8*(4), e59528. https://doi.org/10.1371/journal.pone.0059528

Bessonnard, S., Mot, L. De, Gonze, D., Barriol, M., Dennis, C., Goldbeter, A., Dupont, G., & Chazaud, C. (2014). Gata6, Nanog and Erk signaling control cell fate in the inner cell mass through a tristable regulatory network. *Development (Cambridge)*, *141*(19), 3637–3648. https://doi.org/10.1242/dev.109678

Bessonnard, S., Vandormael-Pournin, S., Coqueran, S., Cohen-Tannoudji, M., & Artus, J. (2019). PDGF Signaling in Primitive Endoderm Cell Survival Is Mediated by PI3K-mTOR Through p53-Independent Mechanism. *Stem Cells*, *37*(7), 888–898. https://doi.org/10.1002/stem.3008

Bora, P., Gahurova, L., Mašek, T., Hauserova, A., Potěšil, D., Jansova, D., Susor, A., Zdráhal, Z., Ajduk, A., Pospíšek, M., & Bruce, A. W. (2020). p38-MAPK mediated rRNA processing and translation regulation enables PrE differentiation during mouse blastocyst maturation. *BioRxiv*, 2020.11.30.403931. https://doi.org/10.1101/2020.11.30.403931

Bora, P., Gahurova, L., Mašek, T., Hauserova, A., Potěšil, D., Jansova, D., Susor, A., Zdráhal, Z., Ajduk, A., Pospíšek, M., & Bruce, A. W. (2021). p38-MAPK-mediated translation regulation during early blastocyst development is required for primitive endoderm differentiation in mice. *Communications Biology*, *4*(1), 788. https://doi.org/10.1038/s42003-021-02290-z

Bora, P., Thamodaran, V., Šušor, A., & Bruce, A. W. (2019). p38-Mitogen Activated Kinases Mediate a Developmental Regulatory Response to Amino Acid Depletion and Associated Oxidative Stress in Mouse Blastocyst Embryos. *Frontiers in Cell and Developmental Biology*, *7*(November), 276. https://doi.org/10.3389/fcell.2019.00276

Brunet, S., & Verlhac, M. H. (2011). Positioning to get out of meiosis: The asymmetry of division. *Human Reproduction Update*, *17*(1), 68–75.

https://doi.org/10.1093/humupd/dmq044

Casser, E., Israel, S., Witten, A., Schulte, K., Schlatt, S., Nordhoff, V., & Boiani, M. (2017). Totipotency segregates between the sister blastomeres of two-cell stage mouse embryos. *Scientific Reports*, *7*(1), 1–15. https://doi.org/10.1038/s41598-017-08266-6

Chaigne, A., Campillo, C., Gov, N. S., Voituriez, R., Azoury, J., Umaña-Diaz, C., Almonacid, M., Queguiner, I., Nassoy, P., Sykes, C., Verlhac, M.-H., & Terret, M.-E. (2013). A soft cortex is essential for asymmetric spindle positioning in mouse oocytes. *Nature Cell Biology*, *15*(8), 958–966. https://doi.org/10.1038/ncb2799

Chazaud, C., & Yamanaka, Y. (2016). Lineage specification in the mouse preimplantation embryo. *Development*, *143*(7), 1063–1074. https://doi.org/10.1242/dev.128314

Chazaud, C., Yamanaka, Y., Pawson, T., & Rossant, J. (2006). Early lineage segregation between epiblast and primitive endoderm in mouse blastocysts through the Grb2-MAPK pathway. *Developmental Cell*, *10*(5), 615–624. https://doi.org/10.1016/j.devcel.2006.02.020

Cheng, A. M., Saxton, T. M., Sakai, R., Kulkarni, S., Mbamalu, G., Vogel, W., Tortorice, C. G., Cardiff, R. D., Cross, J. C., Muller, W. J., Pawson, T., & Ls, O. (1998). *Mammalian Grb2 Regulates Multiple Steps in Embryonic Development and Malignant Transformation University of California at Davis*. *95*, 793–803.

Cirillo, P. F., Pargellis, C., & Regan, J. (2002). The non-diaryl heterocycle classes of p38 MAP kinase inhibitors. *Current Topics in Medicinal Chemistry*, *2*(9), 1021–1035. https://doi.org/10.2174/1568026023393390

Cockburn, K., & Rossant, J. (2010). Making the blastocyst: Lessons from the mouse. *Journal of Clinical Investigation*, *120*(4), 995–1003. https://doi.org/10.1172/JCI41229

Cuadrado, A., & Nebreda, A. R. (2010). Mechanisms and functions of p38 MAPK signalling. *Biochemical Journal*, *429*(3), 403–417. https://doi.org/10.1042/BJ20100323

Davidson, S. M., & Morange, M. (2000). Hsp25 and the p38 MAPK pathway are involved in differentiation of cardiomyocytes. *Developmental Biology*, *218*(2), 146–160. https://doi.org/10.1006/dbio.1999.9596

de Vries, W. N., Evsikov, A. V., Haac, B. E., Fancher, K. S., Holbrook, A. E., Kemler, R., Solter, D., & Knowles, B. B. (2004). Maternal β-catenin and E-cadherin in mouse development. *Development*, *131*(18), 4435–4445. https://doi.org/10.1242/dev.01316

Du, Z., & Lovly, C. M. (2018). Mechanisms of receptor tyrosine kinase activation in cancer. *Molecular Cancer*, *17*(1), 1–13. https://doi.org/10.1186/s12943-018-0782-4

Frankenberg, S., Gerbe, F., Bessonnard, S., Belville, C., Pouchin, P., Bardot, O., & Chazaud, C. (2011). Primitive Endoderm Differentiates via a Three-Step Mechanism Involving Nanog and RTK Signaling. *Developmental Cell*, *21*(6), 1005–1013. https://doi.org/10.1016/j.devcel.2011.10.019

Giannatselis, H., Calder, M., & Watson, A. J. (2011). Ouabain stimulates a Na +/K +-ATPase-mediated SFK-activated signalling pathway that regulates tight junction function in the mouse blastocyst. *PLoS ONE*, *6*(8). https://doi.org/10.1371/journal.pone.0023704

Goldberg, B. S., & Ackerman, M. E. (2020). Antibody-mediated complement activation in pathology and protection. *Immunology & Cell Biology*, *98*(4), 305–317. https://doi.org/https://doi.org/10.1111/imcb.12324

Guo, G., Huss, M., Tong, G. Q., Wang, C., Li Sun, L., Clarke, N. D., & Robson, P. (2010). Resolution of Cell Fate Decisions Revealed by Single-Cell Gene Expression Analysis from Zygote to Blastocyst. *Developmental Cell*, *18*(4), 675–685. https://doi.org/10.1016/j.devcel.2010.02.012

Handyside, A. H., & Barton, S. C. (1977). *Evaluation of the technique of immunosurgery for the isolation of inner cell masses from mouse blastocysts*. *37*, 217–226.

Hirate, Y., Hirahara, S., Inoue, K.-I., Suzuki, A., Alarcon, V. B., Akimoto, K., Hirai, T., Hara,

T., Adachi, M., Chida, K., Ohno, S., Marikawa, Y., Nakao, K., Shimono, A., & Sasaki, H. (2013). Polarity-dependent distribution of angiomotin localizes Hippo signaling in preimplantation embryos. *Current Biology : CB*, *23*(13), 1181–1194. https://doi.org/10.1016/j.cub.2013.05.014

Huot, J., Houle, F., Marceau, F., & Landry, J. (1997). Oxidative stress-induced actin reorganization mediated by the p38 mitogen-activated protein kinase/heat shock protein 27 pathway in vascular endothelial cells. *Circulation Research*, *80*(3), 383–392. https://doi.org/10.1161/01.RES.80.3.383

Kang, M., Garg, V., & Hadjantonakis, A. (2017). Lineage Establishment and Progression within the Inner Cell Mass of the Mouse Blastocyst Requires FGFR1 and FGFR2. *Developmental Cell*, *41*(5), 496-510.e5. https://doi.org/10.1016/j.devcel.2017.05.003

Kang, M., Piliszek, A., Artus, J., & Hadjantonakis, A. K. (2013). FGF4 is required for lineage restriction and salt-and-pepper distribution of primitive endoderm factors but not their initial expression in the mouse. *Development (Cambridge)*, *140*(2), 267–279. https://doi.org/10.1242/dev.084996

Kurimoto, K., Yabuta, Y., Ohinata, Y., Ono, Y., Uno, K. D., Yamada, R. G., Ueda, H. R., & Saitou, M. (2006). An improved single-cell cDNA amplification method for efficient high-density oligonucleotide microarray analysis. *Nucleic Acids Research*, *34*(5), e42. https://doi.org/10.1093/nar/gkl050

Li, R., & Albertini, D. F. (2013). The road to maturation: somatic cell interaction and self-organization of the mammalian oocyte. *Nature Reviews Molecular Cell Biology*, *14*(3), 141–152. https://doi.org/10.1038/nrm3531

Lorthongpanich, C., Messerschmidt, D. M., Chan, S. W., Hong, W., Knowles, B. B., & Solter, D. (2013). Temporal reduction of LATS kinases in the early preimplantation embryo prevents ICM lineage differentiation. *Genes and Development*, *27*(13), 1441–1446. https://doi.org/10.1101/gad.219618.113

Menchero, S., Rayon, T., Andreu, M. J., & Manzanares, M. (2017). Signaling pathways in mammalian preimplantation development: Linking cellular phenotypes to lineage decisions. *Developmental Dynamics*, *246*(4), 245–261. https://doi.org/10.1002/dvdy.24471

Messerschmidt, D. M., & Kemler, R. (2010). Nanog is required for primitive endoderm formation through a non-cell autonomous mechanism. *Developmental Biology*, *344*(1), 129–137. https://doi.org/10.1016/j.ydbio.2010.04.020

Mihajlović, A. I., & Bruce, A. W. (2017). The first cell-fate decision of mouse preimplantation embryo development: integrating cell position and polarity. *Open Biology*, *7*(11). https://doi.org/10.1098/rsob.170210

Mogessie, B., & Schuh, M. (2017). Actin protects mammalian eggs against chromosome segregation errors. *Science*, *357*(6353), eaal1647. https://doi.org/10.1126/science.aal1647

Molotkov, A., Mazot, P., Brewer, J. R., Cinalli, R. M., & Soriano, P. (2017). Distinct Requirements for FGFR1 and FGFR2 in Primitive Endoderm Development and Exit from Pluripotency. *Developmental Cell*, *41*(5), 511-526.e4. https://doi.org/10.1016/j.devcel.2017.05.004

Natale, D. R., Paliga, A. J. M., Beier, F., D'Souza, S. J. A., & Watson, A. J. (2004). p38 MAPK signaling during murine preimplantation development. *Developmental Biology*, *268*(1), 76–88. https://doi.org/10.1016/j.ydbio.2003.12.011

Nichols, J., Silva, J., Roode, M., & Smith, A. (2009). *Suppression of Erk signalling promotes ground state pluripotency in the mouse embryo*. *3222*, 3215–3222. https://doi.org/10.1242/dev.038893

Nishioka, N., Inoue, K. ichi, Adachi, K., Kiyonari, H., Ota, M., Ralston, A., Yabuta, N., Hirahara, S., Stephenson, R. O., Ogonuki, N., Makita, R., Kurihara, H., Morin-Kensicki, E. M., Nojima, H., Rossant, J., Nakao, K., Niwa, H., & Sasaki, H. (2009). The Hippo Signaling Pathway Components Lats and Yap Pattern Tead4 Activity to Distinguish Mouse Trophectoderm from Inner Cell Mass. *Developmental Cell*, *16*(3), 398–410.

https://doi.org/10.1016/j.devcel.2009.02.003

Ohnishi, Y., Huber, W., Tsumura, A., Kang, M., Xenopoulos, P., Kurimoto, K., Oleå, A. K., Araúzo-Bravo, M. J., Saitou, M., Hadjantonakis, A. K., & Hiiragi, T. (2014). Cell-to-cell expression variability followed by signal reinforcement progressively segregates early mouse lineages. *Nature Cell Biology*, *16*(1), 27–37. https://doi.org/10.1038/ncb2881

Petersen, L. K., Blakskjær, P., Chaikuad, A., Christensen, A. B., Dietvorst, J., Holmkvist, J., Knapp, S., Kořínek, M., Larsen, L. K., Pedersen, A. E., Röhm, S., Sløk, F. A., & Hansen, N. J. V. (2016). Novel p38α MAP kinase inhibitors identified from yoctoReactor DNA-encoded small molecule library. *MedChemComm*, *7*(7), 1332–1339. https://doi.org/10.1039/c6md00241b

Plusa, B., Piliszek, A., Frankenberg, S., Artus, J., & Hadjantonakis, A.-K. (2008). Distinct sequential cell behaviours direct primitive endoderm formation in the mouse blastocyst. *Development (Cambridge, England)*, *135*(18), 3081–3091. https://doi.org/10.1242/dev.021519

Posfai, E., Petropoulos, S., de Barros, F. R. O., Schell, J. P., Jurisica, I., Sandberg, R., Lanner, F., & Rossant, J. (2017). Position- and Hippo signaling-dependent plasticity during lineage segregation in the early mouse embryo. *ELife*, *6*. https://doi.org/10.7554/eLife.22906

Remy, G., Risco, A. M., Iñesta-Vaquera, F. A., González-Terán, B., Sabio, G., Davis, R. J., & Cuenda, A. (2010). Differential activation of p38MAPK isoforms by MKK6 and MKK3. *Cellular Signalling*, *22*(4), 660–667. https://doi.org/10.1016/j.cellsig.2009.11.020

Rosàs-canyelles, E., Modzelewski, A. J., Geldert, A., He, L., & Herr, A. E. (2020). *Assessing heterogeneity among single embryos and single blastomeres using open microfluidic design*. 1–14.

Ryan, A. Q., Chan, C. J., Graner, F., & Hiiragi, T. (2019). Lumen Expansion Facilitates Epiblast-Primitive Endoderm Fate Specification during Mouse Blastocyst Formation. *Developmental Cell*, *51*(6), 684-697.e4. https://doi.org/10.1016/j.devcel.2019.10.011

Schrode, N., Saiz, N., Di Talia, S., & Hadjantonakis, A. K. (2014). GATA6 levels modulate primitive endoderm cell fate choice and timing in the mouse blastocyst. *Developmental Cell*, *29*(4), 454–467. https://doi.org/10.1016/j.devcel.2014.04.011

Shuguo, Sun; Kenneth, D. I. (2016). Cellular Organization and Cytoskeletal Regulation of the Hippo Signaling Network. *Trends in Cell Biology*, *26*(9), 694–704. https://doi.org/10.1016/j.tcb.2016.05.003

Silva, J., Nichols, J., Theunissen, T. W., Guo, G., van Oosten, A. L., Barrandon, O., Wray, J., Yamanaka, S., Chambers, I., & Smith, A. (2009). Nanog Is the Gateway to the Pluripotent Ground State. *Cell*, *138*(4), 722–737. https://doi.org/10.1016/j.cell.2009.07.039

Suwińska, A., Czołowska, R., Ozdzeński, W., & Tarkowski, A. K. (2008). Blastomeres of the mouse embryo lose totipotency after the fifth cleavage division: expression of Cdx2 and Oct4 and developmental potential of inner and outer blastomeres of 16- and 32-cell embryos. *Developmental Biology*, *322*(1), 133–144. https://doi.org/10.1016/j.ydbio.2008.07.019

Thamodaran, V., & Bruce, A. W. (2016). p38 (Mapk14/11) occupies a regulatory node governing entry into primitive endoderm differentiation during preimplantation mouse embryo development. *Open Biology*, *6*(9), 15034. https://doi.org/10.1098/rsob.160190

White, M. D., Zenker, J., Bissiere, S., & Plachta, N. (2018). Instructions for Assembling the Early Mammalian Embryo. *Developmental Cell*, *45*(6), 667–679. https://doi.org/10.1016/j.devcel.2018.05.013

Wicklow, E., Blij, S., Frum, T., Hirate, Y., Lang, R. A., Sasaki, H., & Ralston, A. (2014). HIPPO pathway members restrict SOX2 to the inner cell mass where it promotes ICM fates in the mouse blastocyst. *PLoS Genetics*, *10*(10), e1004618. https://doi.org/10.1371/journal.pgen.1004618

Wigger, M., Kisielewska, K., Filimonow, K., Plusa, B., Maleszewski, M., & Suwińska, A. (2017). *Plasticity of the inner cell mass in mouse blastocyst is restricted by the activity of FGF / MAPK pathway*. 1–13. https://doi.org/10.1038/s41598-017-15427-0

Yamanaka, Y., Lanner, F., & Rossant, J. (2010). FGF signal-dependent segregation of primitive endoderm and epiblast in the mouse blastocyst. *Development*, *137*(5), 715–724. https://doi.org/10.1242/dev.043471

Yi, K., Rubinstein, B., Unruh, J. R., Guo, F., Slaughter, B. D., & Li, R. (2013). Sequential actin-based pushing forces drive meiosis I chromosome migration and symmetry breaking in oocytes. *Journal of Cell Biology*, *200*(5), 567–576. https://doi.org/10.1083/jcb.201211068

Zernicka-Goetz, M., Morris, S. A., & Bruce, A. W. (2009). Making a firm decision: multifaceted regulation of cell fate in the early mouse embryo. *Nature Reviews Genetics*, *10*(7), 467–477. https://doi.org/10.1038/nrg2564